

NASA CR-132625

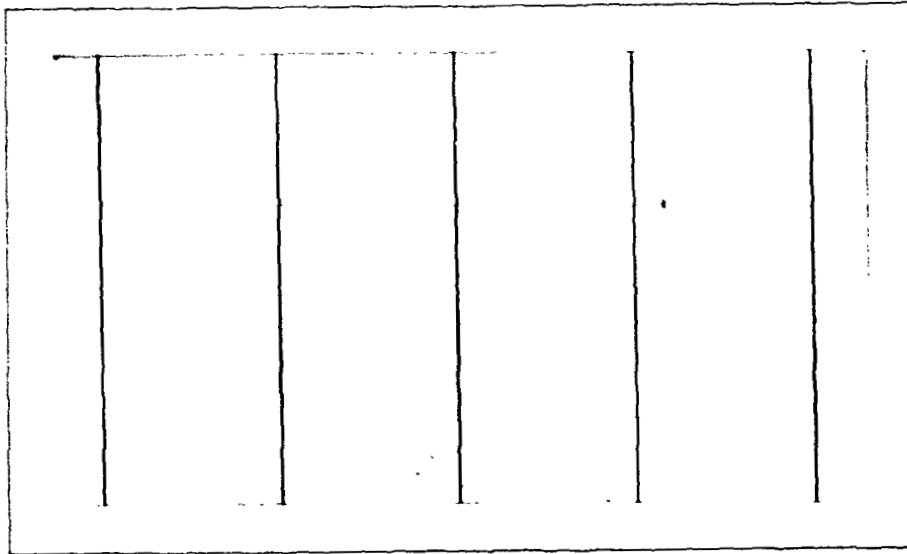
(NASA-CR-132625) OUR CONTAMINATED
ATMOSPHERE: THE DANGER OF CLIMATE CHANGE,
PHASES 1 AND 2 Final Report (Drexel Univ.)
76 p HC \$4.75

N75-28562

CSCI 13E

Unclas
31372

G3/45



EARTH ENERGY EXPERIMENT (E³) PROJECT

NASA CONTRACT NAS 1-11871

drexel university
PHILADELPHIA, PENNSYLVANIA 19104



DEPARTMENT OF PHYSICS
AND ATMOSPHERIC SCIENCE

NASA CR-132625

**OUR CONTAMINATED ATMOSPHERE -
THE DANGER OF CLIMATE CHANGE**

**By Alan J. Cimorelli and
Frederick B. House**

**Final Report
Phases I and II**

**Prepared under Contract No. NAS1-11871 by
Department of Physics and Atmospheric Science
Drexel University
Philadelphia, Pennsylvania 19104**

for

NATIONAL AERONAUTICS AND SPACE ADMINISTRATION

FOREWORD

The present report is a Master's research paper prepared for the Environmental Science Department at Drexel University. This effort was partially supported by the Langley Research Center under Contract No. NAS1-11871, whose effort is directed towards an investigation of ESSA VII Satellite radiation data for use in long-term earth energy experiments. This report is one of three companion reports which together constitute the final report of phases I and II of subject contract. The other two reports are entitled; "An Investigation of ESSA VII Radiation Data for Use in Long-Term Earth Energy Experiments," published as NASA CR-132623, and "Steady-State Solution to the Conduction Problem of a Spherical Balloon Radiometer," published as NASA CR-132624.

ABSTRACT

Changes in average global and hemispheric surface temperature are related to climate change. The effects of increased concentrations of atmospheric particulate matter on average surface temperature and on the components of the earth's radiation budget are studied. To evaluate these effects, Sellers' (1973) model, which couples particulate loading to surface temperature and to changes in the earth's radiation budget was used. A determination of the feasibility of using satellites to monitor the effect of increased atmospheric particulate concentrations is performed. The principal findings of this study are:

- 1) A change in man-made particulate loading of a factor of 4 is sufficient to initiate an ice-age.
- 2) Variations in the global and hemispheric weighted averages of surface temperature, reflected radiant flux and emitted radiant flux are non-linear functions of particulate loading.
- 3) Zonal variations in reflected and emitted radiant fluxes are linear functions of particulate loading in mid-latitudes and non-linear functions in higher latitudes.
- 4) In order to detect changes in man-made particulate loading of a factor of 2 it was found necessary to sense changes in reflected and emitted radiant fluxes of 2.6 and 0.8 w/m^2 ,

respectively. This corresponds to changes in the equilibrium temperature of the monitoring instrument (black sphere) of -0.2°K (a sensitivity of one part in 1000) for night time measurements and $+0.1^{\circ}\text{K}$ (a sensitivity of 1 part in 3000) for day time measurements.

- 5) It was found that a black satellite sphere proposed by House and Sweet meets the requirement of night time measurement sensitivity, but falls short of the required day time sensitivity. However, non-black, spherical radiometers whose external optical properties are sensitive to either the reflected radiant flux or the emitted radiant flux can meet the observational sensitivity requirements.

ACKNOWLEDGMENTS

I wish to express my appreciation to Dr. Frederick B. House for his encouragement and guidance through this work, and to Dr. W. D. Sellers for supplying me with the data necessary to complete this study.

My sincere thanks and appreciation also go to the excellent staff of the Environmental Engineering and Science Department at Drexel University for providing my graduate education.

A portion of this study was supported by the Langley Research Center of NASA under Contract No. NAS1-11871.

I would also like to express sincere thanks to Mrs. Diane Hanson for her much needed help in the typing of this report.

TABLE OF CONTENTS

	Page
FOREWARD	i
ABSTRACT	ii
ACKNOWLEDGMENTS.	iv
TABLE OF CONTENTS.	v
LIST OF TABLES.	vii
LIST OF FIGURES.	ix
LIST OF SYMBOLS.	x
I. INTRODUCTION.	1
II. BACKGROUND	6
2.1 Earth's Radiation Budget	6
2.2 Global Climate Models - Developmental Summary	7
2.3 Global Climate Models - Futuristic Projections	12
2.4 Effects of Particulates and Carbon Dioxide on Climate.	13
2.5 Monitoring Particulate Loading	15
III. APPROACH.	17
IV. RESULTS.	20
4.1 Zonal Variations in Earth Radiation Budget Components with Particulate Loading.	21
4.2 Variations in Global and Hemispheric Weighted Averages of Earth Radiation Budget Components with Particulate Loading	28
4.3 The Feasibility of Monitoring the Effect of Increased Global Particulate Concentrations.	36

	Page
V. CONCLUSIONS	39
APPENDICIES	
A. Tabulated Data - Zonal Variation in Solar Constant with Month of Year and Zonal Variation in Net Radiation with Particulate Loading	41
B. Tabulated Data - Zonal Variations in Emitted and Reflected Radiant Fluxes with Particulate Loading	49
C. Tabulated Data - Variations in Global and Hemispheric Weighted Averages of Surface Temperature, Emitted and Reflected Radiant Fluxes with Particulate Loading	54
D. Computer Program.	58
REFERENCES.	63
ADDITIONAL BIBLIOGRAPHY	64

LIST OF TABLES

<u>TABLE</u>		<u>PAGE</u>
A1	The variation of Incident Solar Radiation with Latitude for Each Month	42
A2	The Zonal Variation of Net-Radiation with Particulate Loading for January	43
A3	The Zonal Variation of Net-Radiation with Particulate Loading for July	44
A4	The Zonal Variation of Average Surface Temperature with Particulate Loading for January	45
A5	The Zonal Variation of Average Surface Temperature with Particulate Loading for July	46
A6	The Zonal Variation of Albedo with Particulate Loading for January	47
A7	The Zonal Variation of Albedo with Particulate Loading for January	48
B1	The Zonal Variation of Emitted Radiant Flux with Particulate Loading for January	50
B2	The Zonal Variation of Emitted Radiant Flux with Particulate Loading for January	51
B3	The Zonal Variation of Reflected Radiant Flux with Particulate Loading for January	52
B4	The Zonal Variation of Reflected Radiant Flux with Particulate Loading for July	53
C1	Global and Hemispheric Weighted Averages of Surface Temperature with Particulate Loading for January	55
C2	Global and Hemispheric Weighted Averages of Surface Temperature with Particulate Loading for July	55

<u>TABLE</u>		<u>PAGE</u>
C3	Global and Hemispheric Weighted Averages of Emitted Radiant Flux with Particulate Loading for January	56
C4	Global and Hemispheric Weighted Averages of Emitted Radiant Flux with Particulate Loading for July	56
C5	Global and Hemispheric Weighted Averages of Reflected Radiant Flux with Particulate Loading for January	57
C6	Global and Hemispheric Weighted Averages of Reflected Radiant Flux with Particulate Loading for July	57

LIST OF FIGURES

<u>Figure</u>		<u>Page</u>
1.	The Mean Annual Heat Budget of the Northern Hemisphere (London, 1957)	8
2.	Radiant Energy Balance on an Earth Surface Element	9
3.	Zonal Reflected Radiant Flux for January vs. Particulate Loading	22
4.	Zonal Reflected Radiant Flux for July vs. Particulate Loading	23
5.	Zonal Emitted Radiant Flux for January vs. Particulate Loading	24
6.	Zonal Emitted Radiant Flux for July vs. Particulate Loading	25
7.	Zonal Albedo for January vs. Particulate Loading	26
8.	Zonal Albedo for July vs. Particulate Loading	27
9.	Global and Hemispheric Average Surface Temperatures for January v.s. Particulate Loading	29
10.	Global and Hemispheric Average Surface Temperatures for July v.s. Particulate Loading	30
11.	Global and Hemispheric Average Reflected Radiant Flux for January v.s. Particulate Loading	31
12.	Global and Hemispheric Average Reflected Radiant Flux for July v.s. Particulate Loading	32
13.	Global and Hemispheric Average Emitted Radiant Flux for January v.s. Particulate Loading	34
14.	Global and Hemispheric Average Emitted Radiant Flux for July v.s. Particulate Loading	35

LIST OF SYMBOLS

<u>Symbol</u>	<u>Meaning</u>	<u>Page Where First Used</u>
Q_n	Net Radiation	7
H	Irradiance, that is the energy per unit time and area arriving at a surface, w/m^2	7
H_0	Solar Irradiance, w/m^2	7
W_r	Reflected radiant flux	7
W_e	Emitted radiant flux	7
A	Planetary albedo, the fraction of the incident solar irradiance reflected from the earth on a specific space scale	7
ϕ	Angle between solar vector and normal to an earth or satellite surface element	
HA	Hemispheric weighted average	18
GA	Global weighted average	18
X	Variable parameter representing surface temperature, W_e or W_r	18
NHA	Northern hemispheric weighted average	18
SHA	Southern hemispheric weighted average	18
h	Latitude increment = 0, 10, 20, . . . , 80	18
T	Equilibrium temperature of satellite instrument	19
F_{s-s}	Radiation Shape Factor from satellite to sun	19
F_{s-e}	Radiation shape factor from satellite to earth	19
σ	Stefan-Boltzmann constant	19
η	Nadir Angle of satellite	19

Subscripts

E	Earth, earth emitted
R	reflected
S	Solar

Superscripts

i	particulate loading
j	latitude zone
k	time of year

I. INTRODUCTION

In recent years there has been much concern voiced as to the effect of man's activities on his health and his environment. Most of the effect, thus far, has been concentrated in those areas which directly affect his local environment; namely, the effect of increased ambient concentrations of SO₂, NO_x, CO₂, CO, particulate matter, toxic trace metals, etc. The effect of such pollutants on man's health, and the local ecology has been researched to the point where criteria are available by which standards for allowable ambient concentrations can be set.

Such standards are useful only if these concentrations can be effectively monitored so that a potential problem can be detected and corrected before it becomes a reality. For such local pollutant problems, effective ambient and source monitoring systems have been developed. Most techniques involve taking a small sample of air and chemically analyzing it in order to determine relative pollutant concentrations and then generalizing to a small local environment. Although these local pollutant problems are a threat to man's well-being, they are reasonably understood and effectively monitored. Such environmental problems, at least for the time being, manifest themselves in enforcement.

The area in which comparatively little concrete data exists for both determining environmental effects and developing reasonable

monitoring techniques is man's effect on the global environment. Here there is a great deal of somewhat questionable evidence which suggests that due to man's activities, changes in the global environment may occur which will drastically threaten our life styles, if not our very existence. Specifically, has man inadvertently changed the global climate, or is he about to do so?

It is necessary, according to Lorenz (1970) to first determine whether or not climate changes have occurred, and if so, their nature and extent. In order to deal with this problem in a complete way, it would be necessary to develop a means by which we could identify small trends in the characteristics in a widely random varying atmosphere. Although such a complete solution is not presently available, the evidence of climate change exists. History has recorded vegetation changes, in a particular locale, of a type which must have been caused by a dramatic change in rainfall or temperature. For example, the great oil fields of Alaska, which were produced by vast amounts of organic matter, indicate that at the time of their inception, a climate much different from that of the present must have existed. Most striking is the advance and retreat of the prehistoric continental glaciers. These glacial epochs indicate large oscillations in the global climate, having periods in the order of millions of years.

Aside from such long-term changes, there is also evidence which indicates climate changes occurring in contemporary history. Mitchell (1971) among others, claims that during the last century a systematic

fluctuation of global climate is revealed by meteorological data. He states that between 1880 and 1940 a net warming of about 0.6°C occurred, and from 1940 to the present our globe experienced a net cooling of 0.3°C .

Once such changes have been established it is necessary that their causes and effects be identified. Towards this end a large number of variables which describe our climate must be identified and their relative importance assessed. Since this is such a large task, models which grossly parameterize these variables are developed, solved and perturbed.

The effect occurring due to a climate change could be as mild as a slight inconvenience caused by hotter summers or as devastating as the annihilation of northern civilizations by the intrusion of massive continental ice sheets. The effect is purely a matter of the magnitude of the climate change.

The possibility exists, according to some authors, that our climate is intransitive. That is, small perturbations occurring in certain atmospheric variables may cause our climate to change to a new steady state climate. Quantities such as the amount of solar radiation received by the planet per unit area per unit time (solar irradiance), the total reflectivity of the earth-atmosphere system (albedo), and the concentrations of atmospheric constituents which affect the radiative transfer characteristics of the atmosphere (specifically; CO_2 and particulate matter) are variables of this type.

Immediately the question arises, is man in a position to affect these quantities and if so to what degree and with what resulting effect? Obviously man has no control over the incident solar irradiance. He can but monitor it and speculate on possible climate change which would occur if it varied. Fortunately, this solar radiation averaged over a period of time is constant and there is little evidence which would suggest its changing. In recent years there has been much data collected which indicates that the global concentrations of both CO₂ and particulate matter, through man's industrial activities, are on an increase.

The effect of increasing global concentrations of CO₂ is to increase the average global surface temperature. This effect is known as the "Greenhouse Effect." It was first suggested by Tyndall in 1863, as reported in the SCEP (Study of Critical Environmental Problems) Work Group, that

" . . . the blanketing effect of increased CO₂ would cause climate changes through variation of the surface temperature. Increased CO₂, because of its strong absorptior (and therefore emission) of infrared radiation at 12 to 18μ, would reradiate surface and further inhibit the radiative cooling at the ground."

As for increasing global concentrations of particulate matter, the opposite is true. Due to the backscattering characteristics of the particles an increase in the albedo occurs which produces a decrease in average global surface temperature.

NASA Langley Research Center in the report "Remote Measurement of Pollution" states,

"Particles affect the transfer of radiation through the atmosphere by virtue of their ability to absorb, emit, and scatter radiation. In the visible portion of the spectrum, the scattering of radiation by particles can equal or exceed the scattering due to the normal gaseous constituents. In some cities the long-term average of solar radiation reaching the ground is reduced by particles by more than 10%."

Since it had been thought that the two effects canceled one another, their use as criteria for developing standards has not been considered. However, it has since been found that the rate of temperature increase decreases with increasing CO₂ and increases with increasing particulates. Therefore, global particulate loading is of foremost concern.

Sellers (1973) has developed a climate model which quantitatively relates particulate loading to surface temperature. He has shown that an increase in man-made global particulates by a factor of 4.0 will initiate an ice-age. In order that we safeguard ourselves and future generations from a self-imposed ice-age it is necessary that we effectively monitor global concentrations of particulate matter.

Using Sellers' data a determination of the feasibility of monitoring the effect of increases in global particulates through the use of existing satellite technology was performed. It was found that earth radiation balance measurements performed by a fleet of proposed satellites are accurate enough to implicitly detect, through earth radiation budget measurements, increases in global particulate concentrations.

II. BACKGROUND

2.1 Earth's Radiation Budget

Consider the earth and atmosphere as an entire system, then at the interface between the earth's atmosphere and space, incoming and outgoing radiation fluxes are the means by which energy is exchanged between the sun and the earth - atmosphere system. The earth receives short wave radiation ($.2\mu$ to 3.5μ) from the sun (insolation). A portion of this radiation is reflected back into space and therefore contributes nothing in the way of available heat energy to the earth-atmosphere system. The remainder of the radiation is absorbed by the earth and atmosphere. This absorbed radiation acts to heat the absorber which in turn reradiates according to Stefan-Boltzmann's Law and at a wavelength consistent with Plank's Law. The earth loses energy (emitted radiation) to space by thermal emittance of longwave radiation at wavelengths greater than 4.0μ . This rate of heat loss must exactly balance over a long period of time the amount of heat received from the sun, in order to prevent the earth from becoming continuously hotter or continuously colder, as the case may be. This energy exchange with space is the radiation balance or net radiation at the top of the atmosphere. Linked to the radiation balance, through thermal exchange mechanisms, is the surface temperature of the earth. It is this parameter which is quantitatively synonymous with climate.

One other pertinent quantity needs to be defined; namely, the albedo. The albedo is the percentage of the insolation which is reflected back into space, i.e. the ratio of the reflected radiation to the insolation.

Figure L shows the mean annual heat budget (radiation balance) of the northern hemisphere. Here is seen the way in which radiation distributes itself within the earth-atmosphere system. The actual quantities appearing in the figure are representative but somewhat out-dated. For example, recent satellite measurements indicate that the albedo is 29 or 30%.

The earth's net radiation budget for any space and time scale is given by:

$$Q_n = H_s - (W_r + W_e)$$

or,

$$Q_n = H_s (1-A) - W_e$$

where,

$$H_s = H_0 \cos \theta$$

Figure 2 describes this situation pictorially.

Satellite experiments are designed to effectively measure emitted radiant flux and albedo on a predetermined space and time scale. In order to generate the global net radiation, the reflected radiant flux is integrated over the entire earth.

2.2 Global Climate Models - Developmental Summary

In order to relate the quantities found in the radiation budget to surface temperature we must specify all those characteristics and

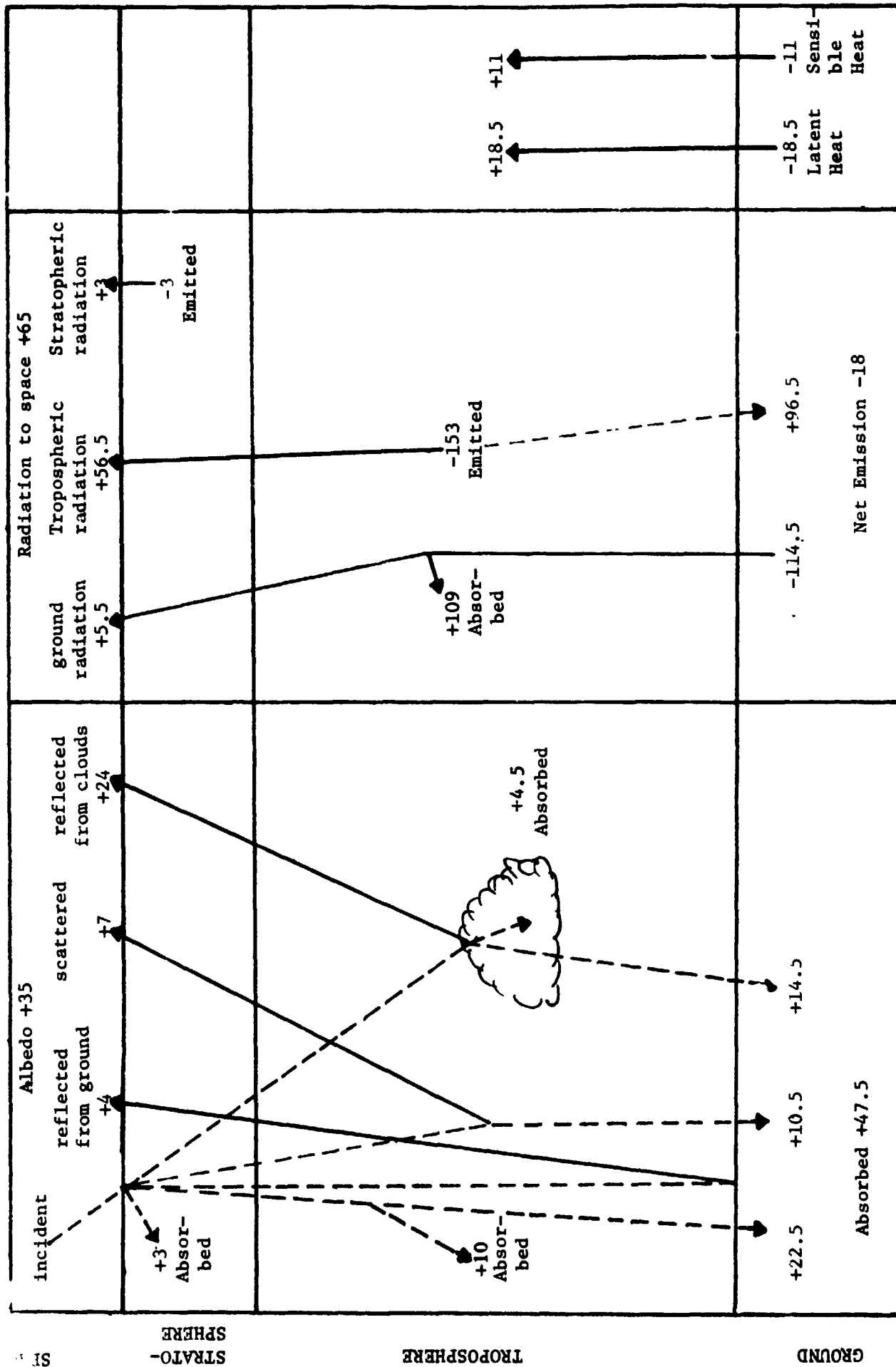


Figure 1: The mean annual heat budget of the Northern Hemisphere, after London.

EARTH RADIATION

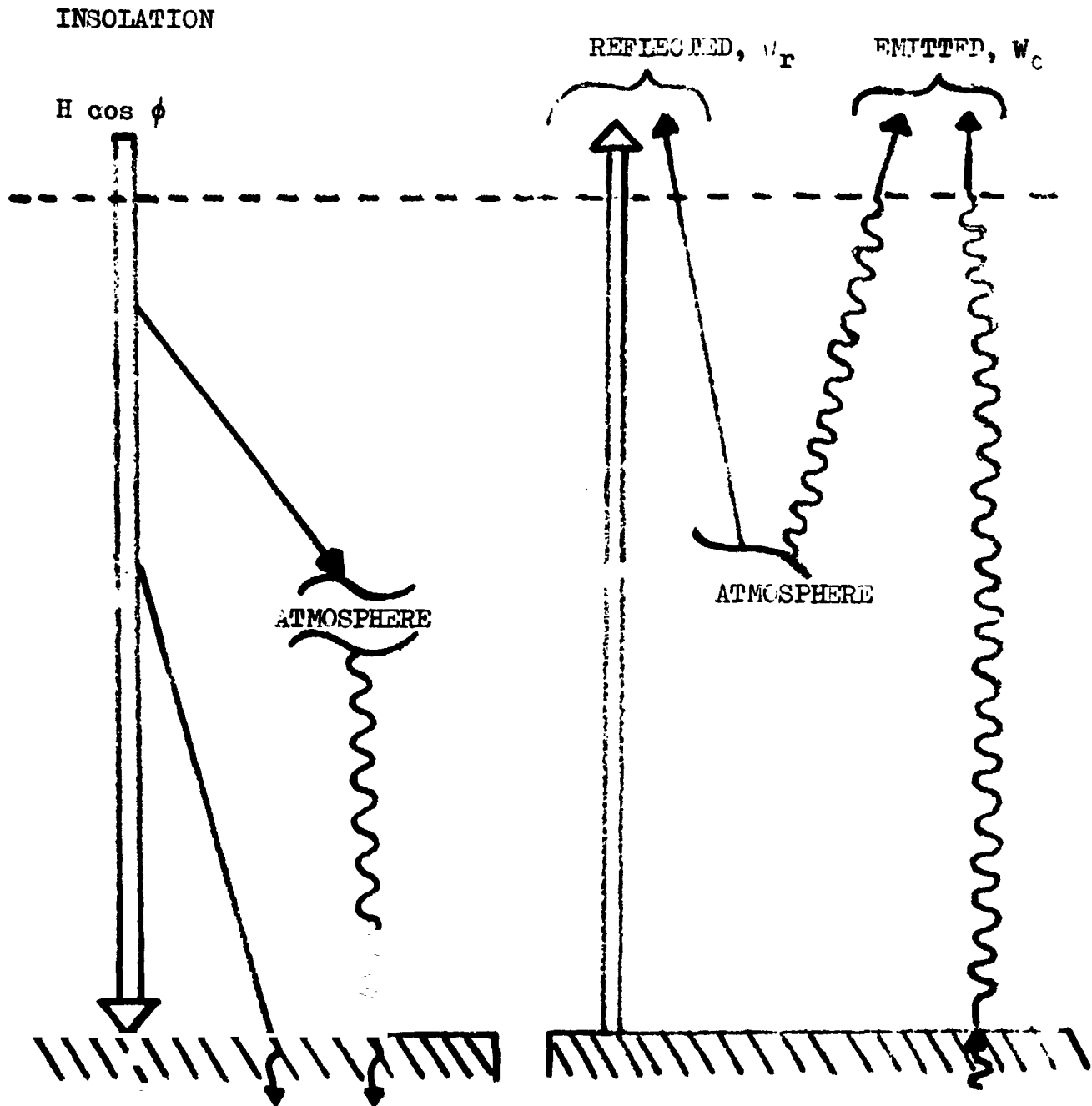


Figure 2: Radiant Energy Balance on an Earth Surface Element

mechanisms which affect heat transfer within the earth-atmosphere system, i.e., atmospheric motions, ground conditions, radiative and connective processes within the atmosphere and atmospheric constituent concentrations. To accomplish this, global climate models are developed. Using the data produced from earth radiation budget measurements as input for a global climate model, surface temperature fields can be generalized. The worth of these models is seen in their ability to reproduce our existing climate using available earth radiation budget data, whereas their merit is in their ability to predict climate change.

In general, global climate models proceed as follows: In order to deal with climate on a mathematical basis, the climate must first be defined as a collection of long-term statistical properties of the atmosphere. Usually five such properties are used: the three dimensional fields of temperature, pressure, density, wind velocity and water in its various forms. Once these properties have been identified the physical laws which govern their variations must be written as mathematical equations. A solution of this set of equations defines the state of the atmosphere at a given instant of time. But, before a solution can be generated the state of the environment must be identified. This can be done in one of two ways. It can be assumed that a knowledge of how the environment will behave is known, in which case environmental factors enter the model as constants. Or we could introduce those characteristics which describe the state of the environment as variables in terms of them. For example, allow

particulate concentrations to enter the model in an equation which relates available solar radiation to environmental factors.

To illustrate this consider the following example. In any global climate model a fundamental quantity which must be determined in order that it be used as input to the model is the amount of solar radiation absorbed by the earth-atmosphere system. This quantity is found by differencing the solar radiant flux incident upon the atmosphere, which is known to be approximately constant (solar constant), and the solar radiant flux reflected by the earth-atmosphere system. Moreover, the reflected radiant flux depends strongly upon environmental conditions such as cloud cover, type of underlying surface and concentration of atmospheric constituents. Specifically, it is well known that the reflected radiant flux is sensitive to atmospheric particulate concentrations; therefore, our climate model must account for such concentrations. This can be accomplished in one of the two ways previously stated, where in this case the environmental factor is atmospheric particulate concentrations and the atmospheric variable is the reflected radiant flux. Once the equations are written and environmental factors considered a solution proceeds as follows:

- 1) In the equations all partial derivatives are replaced by finite differences.
- 2) The initial and boundary conditions are chosen.
- 3) Spacial and temporal increments are chosen.
- 4) The equations are then solved in a step-wise manner with the aid of a digital computer.

Since there is such a large number of variables to be considered, those models which are capable of being completely solved are necessarily quite simple.

2.3 Global Climate Models - Futuristic Projections

Once it has been established that a climate model accounts reasonably well for the present climate it is then used as a speculative tool. This is accomplished by perturbing certain parameters used in the model and examining the resulting climate change. Although such models differ in their treatment, their results are quite similar.

Budyko's model (1970) indicates that a reduction of 1.6% of the solar radiation will produce an ice cover on the globe reaching a mean latitude of 50° . Sellers (1973) found a similar result using his model. He determined that a decrease of 2% in solar radiation would produce ice caps extending to 50° . Most frightening of all is the work done by Faegre (1972): he reports that there are five steady state solutions (global temperature distributions) consistent with his model. One of the solutions corresponds to our present climate while the others represent much different climates. In perturbing each of the solutions he found that our present climate may be unstable and that a decrease of 2% in radiation results in a climate corresponding to an ice-covered earth. Although this result is consistent with the results of Budyko and Sellers, Faegre's model is dissimilar in that it indicates that if the earth is perturbed into an ice-covered climate it will not return to our present climate should the radiation return

to its present value. Even though these models contain a large number of assumptions which grossly simplify the actual systems and for this reason some scientists refute them, they are the best working tool available in the area. Since there is such close agreement among them, it seems quite necessary to determine which atmospheric constituents and or pollutants, controllable by man, are able to affect such climate change. Having identified these constituents, how can we monitor and control their numbers?

2.4 Effect of Particulates and Carbon Dioxide on Climate

It has been well established, in the literature for a number of years, that the two pollutants which possess the greatest possibility of drastically effecting our climate are CO₂ and particulate matter. Up until recently, it was thought that the cooling effect produced by increased concentrations of particulate matter would be canceled by the warming effect of CO₂. But it was found by Rasool and Schneider in 1971 that,

" . . . although the addition of CO₂ in the atmosphere does increase the surface temperature, the rate of temperature increase diminishes with increasing CO₂ in the atmosphere. For aerosols, however, the net effect of increase in density is to reduce the surface temperature of the Earth. Because of the exponential dependence of the backscattering the rate of temperature decrease is augmented with increasing aerosol content."

Their results showed that an increase by a factor of eight of global CO₂ concentrations will produce an increase in surface temperature of less than 2°C, whereas increasing particulate concentrations by a

factor of four could decrease the mean surface temperature as much as 3.5°C. Therefore, as the global concentrations of both CO₂ and particulates are increased, it is the radiative shielding effect of the particulates which plays the dominate role.

Although such an increase in particulate pollution seems quite unlikely, a number of studies indicate that such an occurrence is possible if we continue polluting at our present rate. In a publication prepared by NASA Langley Research Center (1971) continued increasing particulate concentrations are reported, and I quote, "There is little doubt that over many populated areas, atmospheric turbidity is increasing. Solar radiation measurements in Japan and in the European part of the USSR show this increase clearly." McCormick and Ludwig, 1967, presented data which indicated that global turbidity has increased approximately 10 to 20% per decade for the general period of 1910 to 1960. Their data comes from measurements taken from Davos, Switzerland and Washington, D.C. Also, Schaefer's, 1968, measurements taken in the United States, have shown that atmospheric particulate concentrations have increased by at least an order of magnitude in the last ten years. Finally, Ludwig and Morgan, 1970, predict that man's potential to pollute will increase six-to-eight fold in the next fifty years. All of these studies point to the possibility, in the not so distant future, of man polluting himself into an ice-age.

Sellers, 1973, developed a new global climate model which accounts for significant atmospheric variables. He found, upon

analyzing the sensitivity of his model to increased concentrations of CO₂ and particulates, a similar result to that of Rasool and Schneider. He doubled and halved the initial CO₂ content of the atmosphere with no appreciable effect on surface temperature. However, upon analyzing the model's sensitivity to changing concentrations of particulate matter he found surface temperature to drop even more drastically than that predicted by Rasool and Schneider. His model predicts a drop of 0.5°C in global surface temperature by doubling man-made global atmospheric particulate concentrations. And if we increased the amount of man-made particulates by a factor of 3 global surface temperature would decrease 1.3°C. His findings show that the rate of decrease of global surface temperature increases as more particulates are added to the atmosphere. He increased the amount of man-made global particulates as much as six fold which resulted in a global surface temperature drop of 12.5°C. If man is in a position to affect such change then it is certainly the time to reevaluate our priorities.

2.5 Monitoring Particulate Loading

Unlike pollution problems on a local level, the problem of increasing particulate concentrations on a global basis is quite vague in comparison.

The studies and models cited above, by their very nature, do not afford working criteria by which reasonable standards could be set and control implemented. But, since they do indicate the

possibility of such drastic global consequences the implementation of some form of early warning monitoring system is essential.

The only methods available, by which a determination of the ambient concentrations of particulates can be made, are good only for small local areas. Such data is useless for monitoring climate change due to increased particulate concentrations since average global concentrations are needed. Therefore, rather than monitoring these concentrations directly, we could monitor some quantity whose magnitude is quite sensitive to changes in particulate concentrations. One way to accomplish this would be to monitor changes in average global surface temperature since according to Sellers (1973) changes in surface temperature are certainly sensitive enough (see figure 3 and 4). However, the problem with using such a quantity is that our surface sensing devices do not have global extent. And even if an accurate measure could be made by the time we sensed the change it would be unlikely that anything could be done about it. Therefore, a parameter is needed which is first, sensitive enough to changes in atmospheric particulate concentrations, such that its resulting change is within the limits of its measurement, and secondly, can be measured on a global basis. Earth energy budget measurements were found to be of this type.

III. APPROACH

Sellers (1973) reported the variation in average global surface temperature as a function of particulate optical depth. It was necessary to relate these data to what occurs at the top of the atmosphere. That is, those changes in the components of the global radiation budget which must have occurred to produce the reported changes in the average global surface temperature. In order to accomplish this a request was made to Dr. Sellers for the data which were used as input to his model to generate the surface temperature variations. Whereupon data were sent concerning zonal variations in net radiation, albedo as a function of molecular plus particulate optical depth for January and July, and the variation in solar irradiation as a function of latitude for the twelve months.

Using these data it was possible to determine the sensitivity of the short and long wave radiant exstance to changes in global particulate concentrations. Given the net radiation, albedo, solar irradiance for a specific latitude zone, optical depth and time of year, the corresponding emitted and reflected radiant fluxes were calculated as follows:

$$W_e^{ijk} = H_{\theta}^{jk} (1-A^{ijk}) - Q_n^{ij} \quad (1)$$

and

$$W_r^{ijk} = H_{\theta}^{jk} A^{ijk} \quad (2)$$

The sensitivity of reflected and emitted radiant fluxes to changes in the global concentrations of particulate matter was compared to a satellite's sensitivity to changes in the reflected and emitted radiant fluxes. This was done in order to determine the feasibility of using satellites to monitor the effect of increased global concentrations of particulates.

Again, using Sellers' data it was possible to compute the global and hemispherical area-weighted averages for solar reflected radiation and terrestrial emitted radiation for January and July for varying particulate concentrations. The averages were calculated as follows:

$$(HA)^{ik} = \frac{\sum_{j=1}^{9.80} x^{ij} [\sin(90-h) - \sin(80-h)]}{\sum_{h=0}^{80} [\sin(90-h) - \sin(80-h)]}$$

and

$$(GA)^{ik} = \frac{[(NHA)_{ik} + (SHA)_{ik}]}{2 \sum_{h=0}^{80} [\sin(90-h) - \sin(80-h)]}$$

In order to determine whether or not these changes in the earth radiation budget components with particulate loading can be sensed by

the satellite monitoring instrument, it was necessary to compute the changes in equilibrium temperature of the instrument with particulate loading. It is the equilibrium temperature of the instrument which is measured and from which earth radiation budget components are deciphered. These changes in equilibrium temperature were then compared with instrument sensitivity in order to determine the feasibility of using such a monitoring system.

The instrument considered is a metallic spherical detector optically black. The external radiation absorbed by the sphere (the addition of solar incident, solar reflected and terrestrial emitted) produces a proportional internal irradiance that will be detected, as equilibrium temperature, by internally facing radiometers.

The equations used to calculate the equilibrium temperature of the sphere are as follows:

When the sphere is illuminated by the sun (daytime)

$$T = [(F_{s-s} H_{\theta} + F_{s-e} (2W_r + W_e)) / \sigma]^{1/4} \quad (5)$$

When the sphere is in the shadow of the earth (nighttime)

$$T = [(F_{s-e} W_e) / \sigma]^{1/4} \quad (6)$$

where

$$F_{s-s} = .25$$

$$F_{s-e} = \frac{(1 - \cos \eta)}{2} = .2705 \text{ for a sphere at 800 km assuming isotropic conditions.}$$

IV. RESULTS

Through the use of the climate model developed by Sellers (1973) the feasibility of monitoring climate change, i.e. changes in surface temperature, due to increases in global atmospheric particulate concentrations is reported.

It was stated previously that a change in average surface temperature of 3°C is sufficient to initiate an ice age. If the monitoring of climate change is to be a viable tool through which global atmospheric concentrations can be controlled it would be necessary for the monitoring instrument to be able to sense changes in average surface temperature of much less than 3°C . Changes in the order of one-half degree would be meaningful.

Using the data reported in Appendix A global and hemispheric weighted averages and zonal variations in surface temperature, short-wave reflected radiant flux and long-wave emitted radiant flux for January and July as functions of molecular plus particulate optical depth are generated. The results of these computations are found in Appendices B and C. These results are also plotted in Figures 3 through 14.

On the graphs, an optical depth of 0.300 corresponds to the present optical thickness of the clear atmosphere. This consists of the sum of a molecular optical depth of 0.145 and a particulate optical depth

of 0.155. Of the particulate optical depth it is thought that man contributes 0.023, or about 15%. The optical depth was increased by multiples of 0.023 such that upper limit of particulate loading, i.e. 0.415, appearing on the graphs corresponds to an increase in man-made particulate optical depth by a factor of six.

4.1 Zonal Variations in Earth Radiation Budget Components with Particulate Loading

Zonal variations in reflected and emitted radiant fluxes and albedo with particulate loading for January and July are computed. The results of these computations are found in Appendix B. These results are also plotted in Figures 3 through 8.

Figures 3 through 8 show the variations reflected and emitted radiant fluxes and albedo with particulate loading for January and July. The variations are calculated for each 10 degree latitude zone. In the figures the latitude zones of 60-70 north, 30-40 north, 0-10 north, 30-40 south and 60-70 south are reported.

A general characteristic of the graphs is that in the low and middle latitudes the dependence of the reflected radiation stream and albedo on particulate loading is essentially linear whereas the dependence of the emitted radiant flux is non-linearly decreasing. In the higher latitudes the dependence of the reflected and emitted radiant fluxes are found to be non-linearly increasing and decreasing, respectively. These results can be accounted for in the fact that for high latitudes the incident solar radiation encounters a larger atmospheric path than in the low and mid latitudes. Therefore, the radiation stream comes in contact with a larger number of particles which in fact increases the effective optical depth at those latitudes.

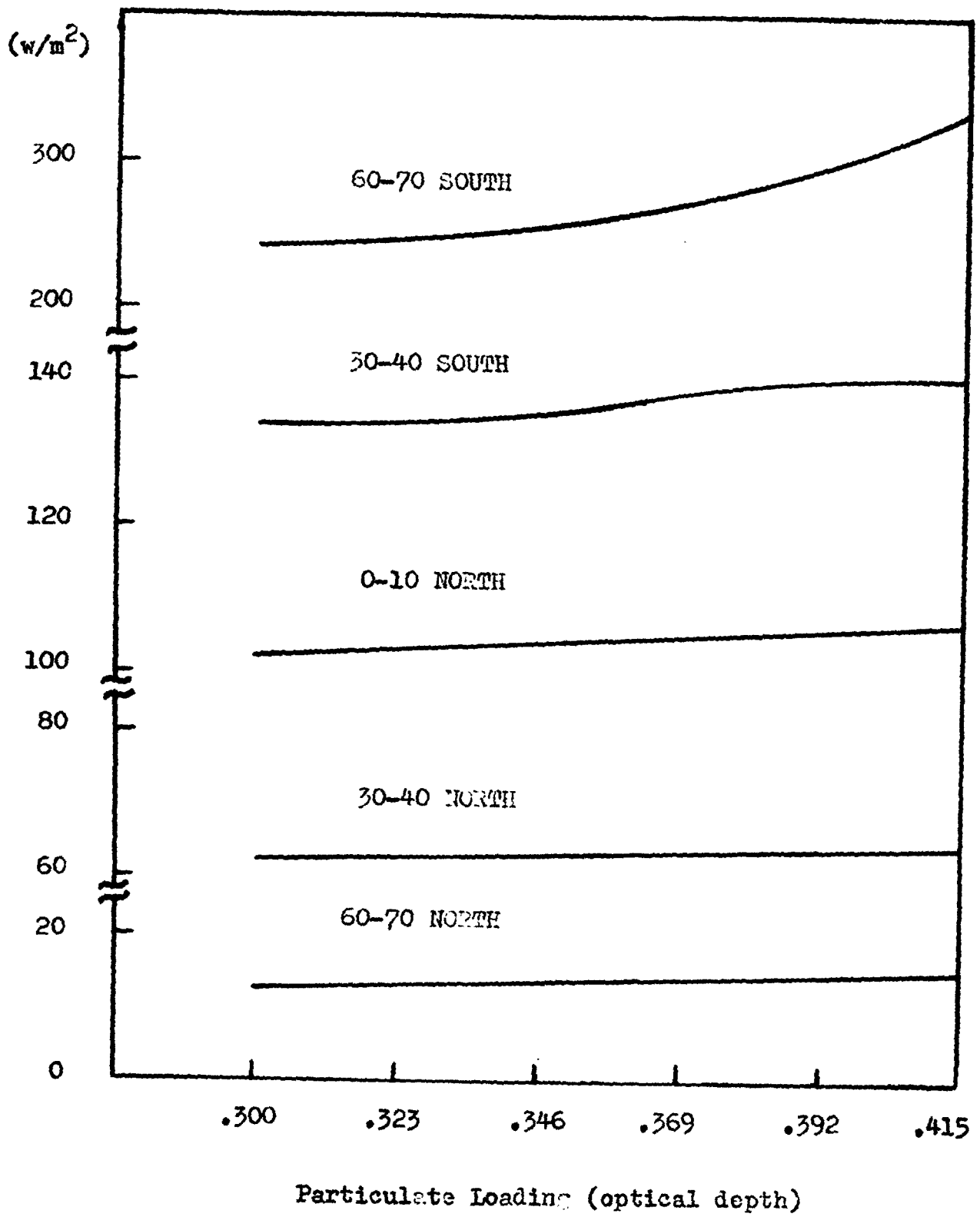


Figure 3. Zonal Reflected Radiant Flux for January vs. Particulate Loading

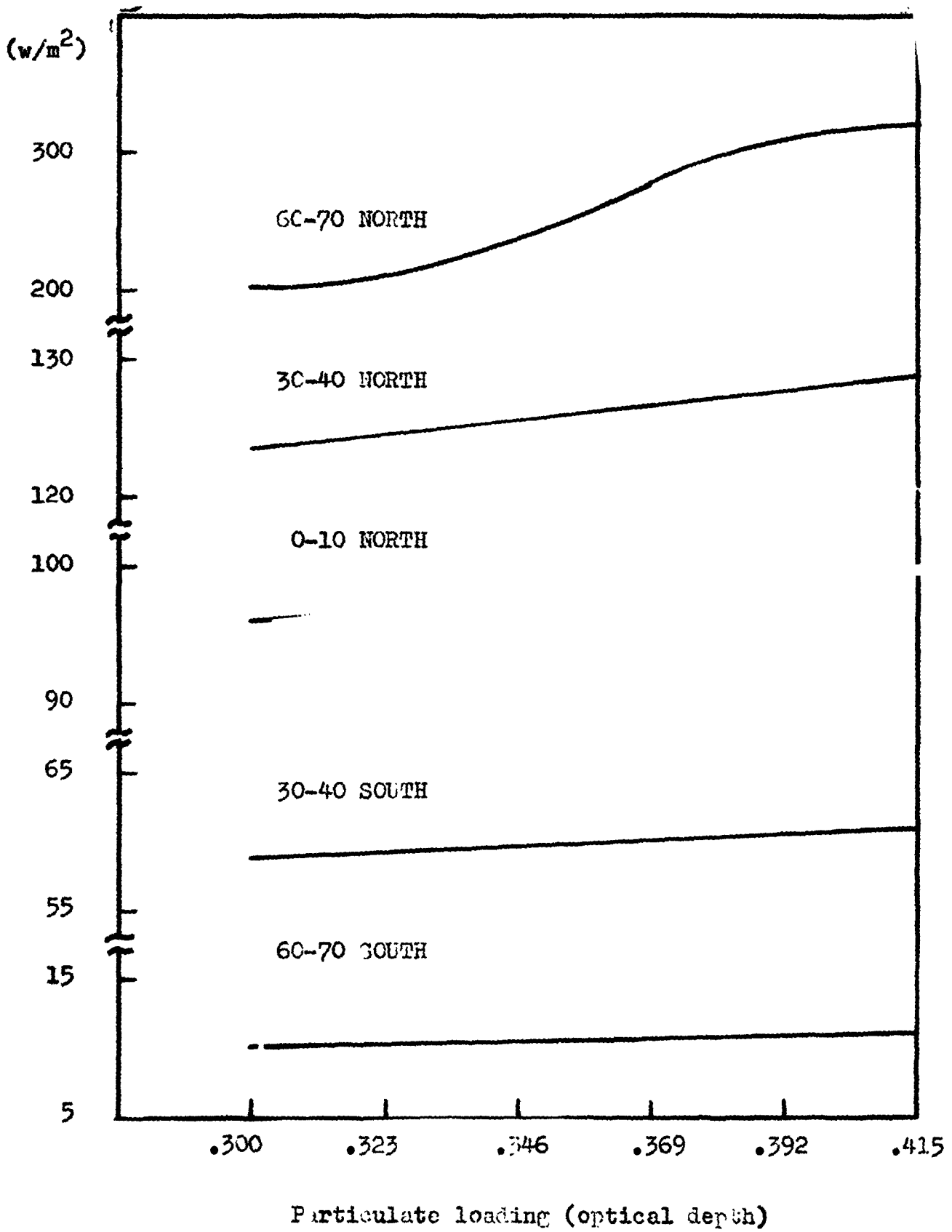


Figure 4. Zonal Reflected Radiant Flux for July vs. Particulate Loading

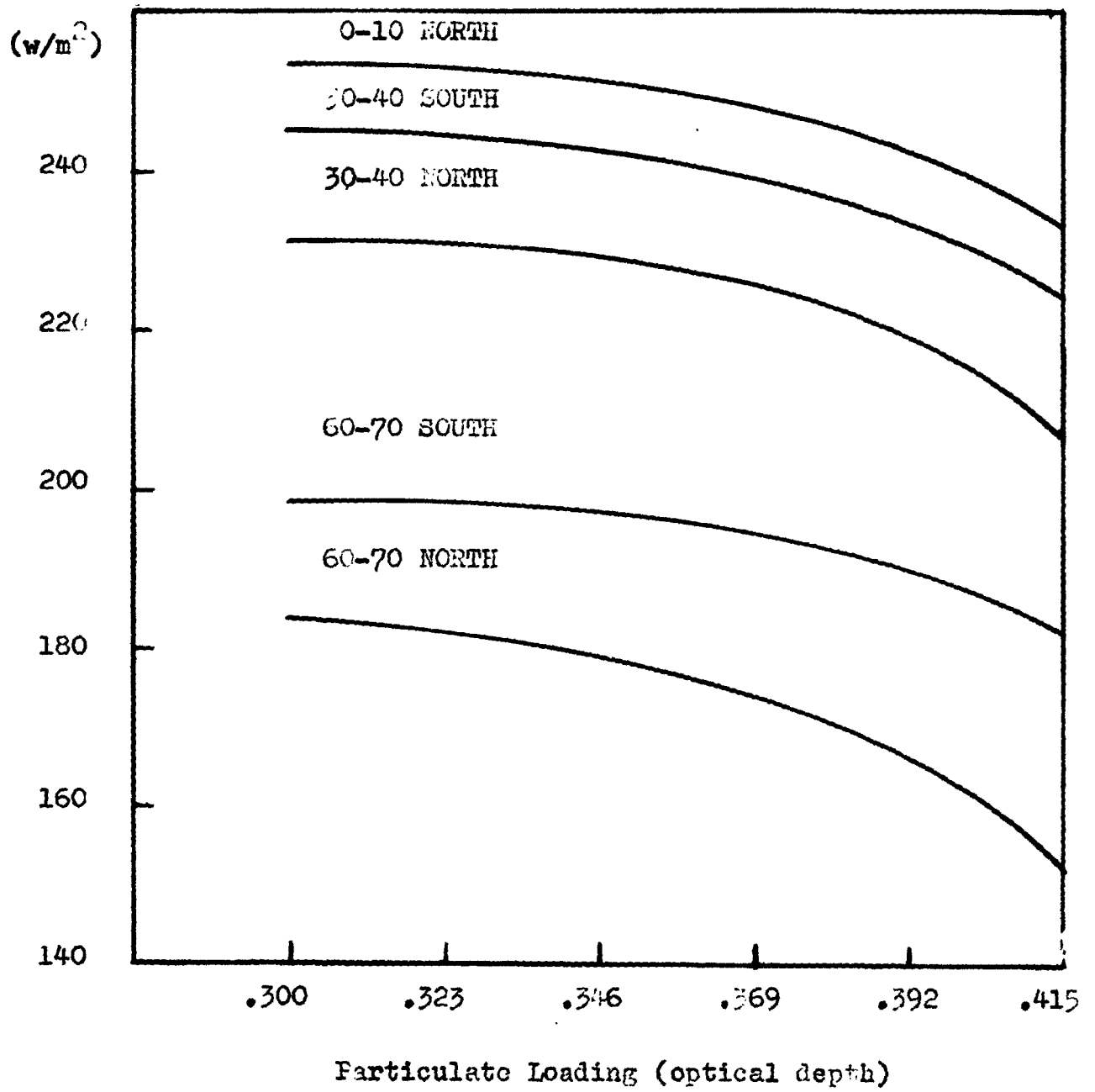


Figure 5. Zonal Emitted Radiant Flux for January vs. Particulate Loading

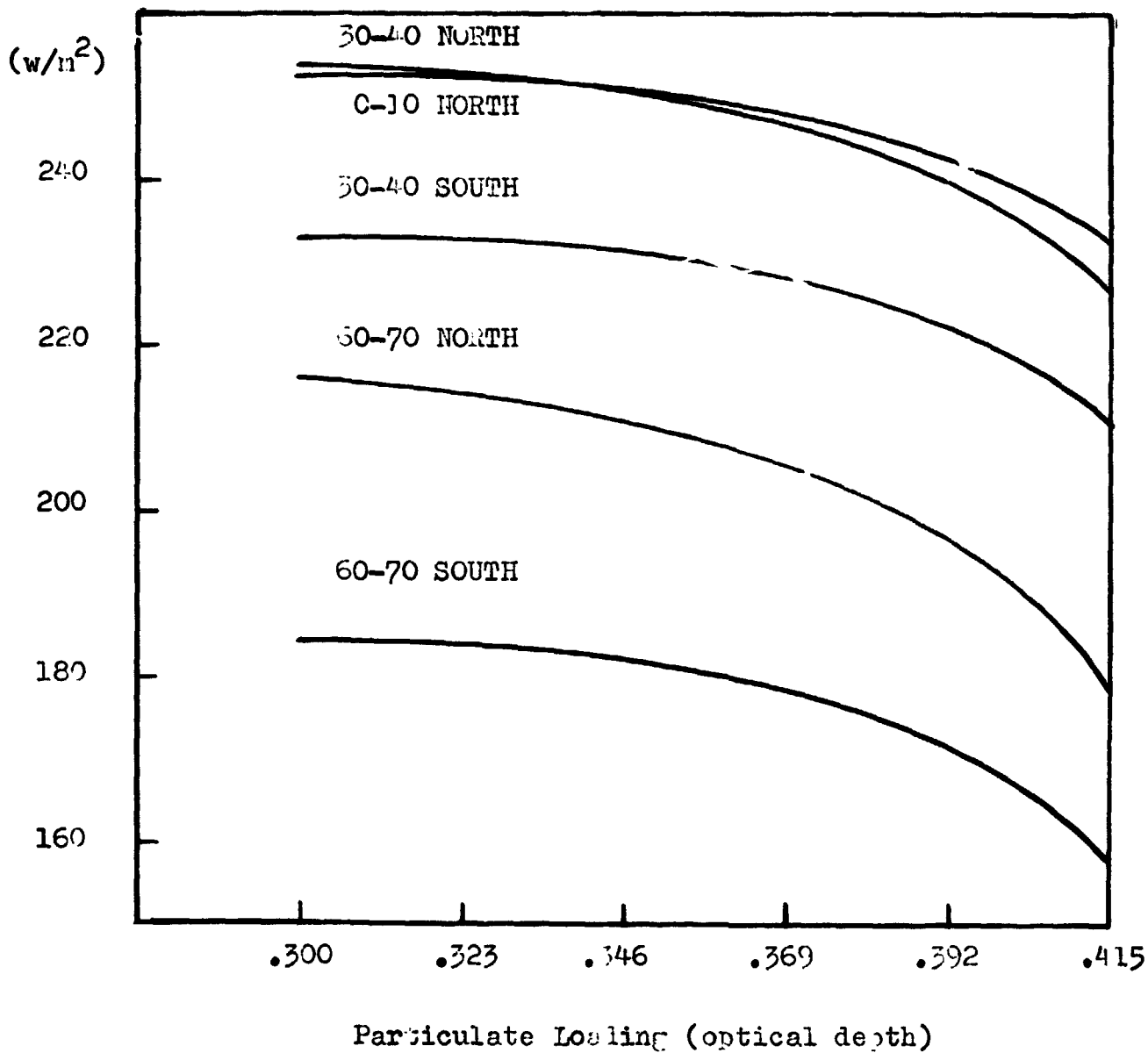


Figure 6. Zonal Emitted Radiant Flux for July vs. Particulate Loading

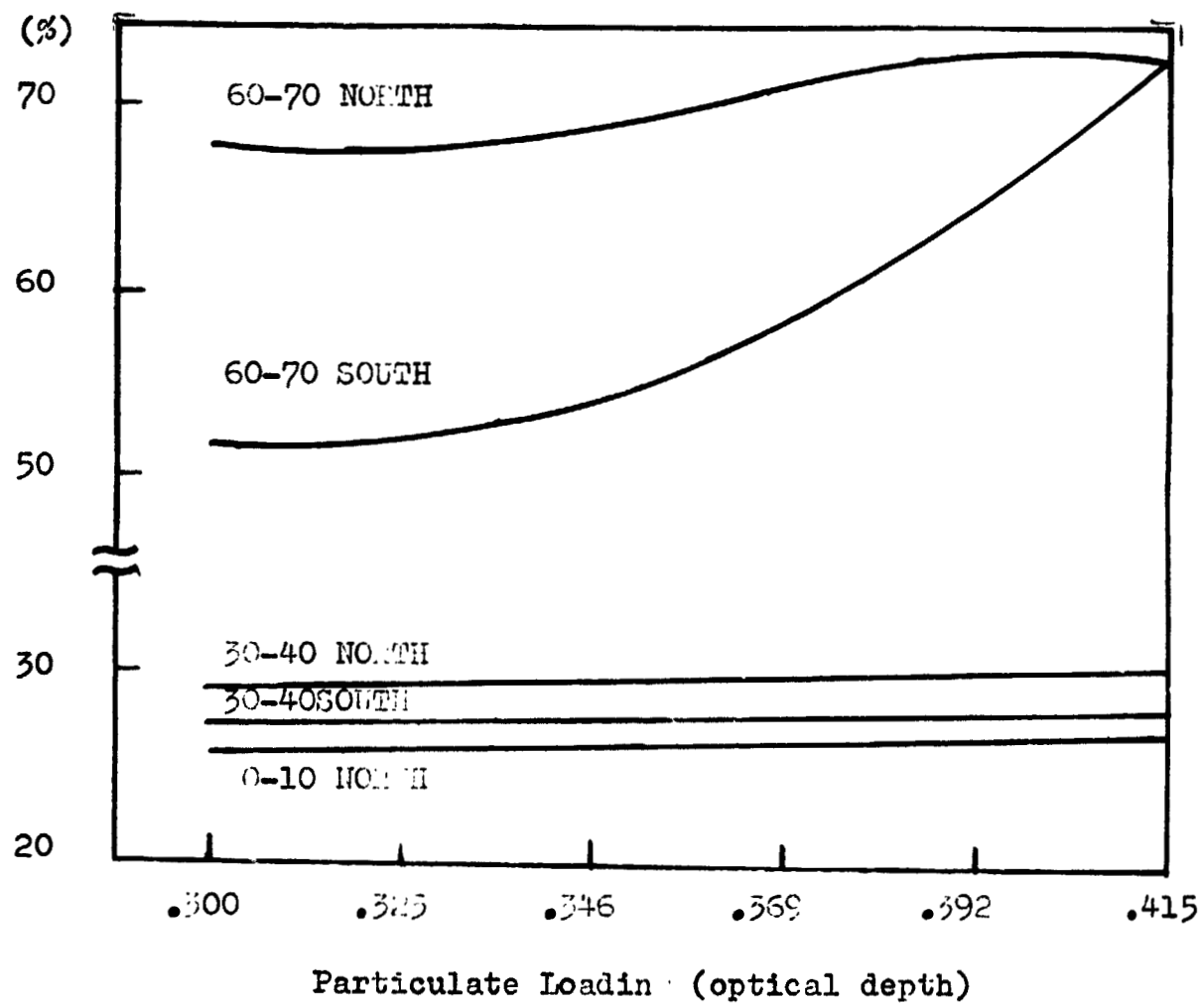


Figure 7. Zonal Albedo for January vs. Particulate Loading

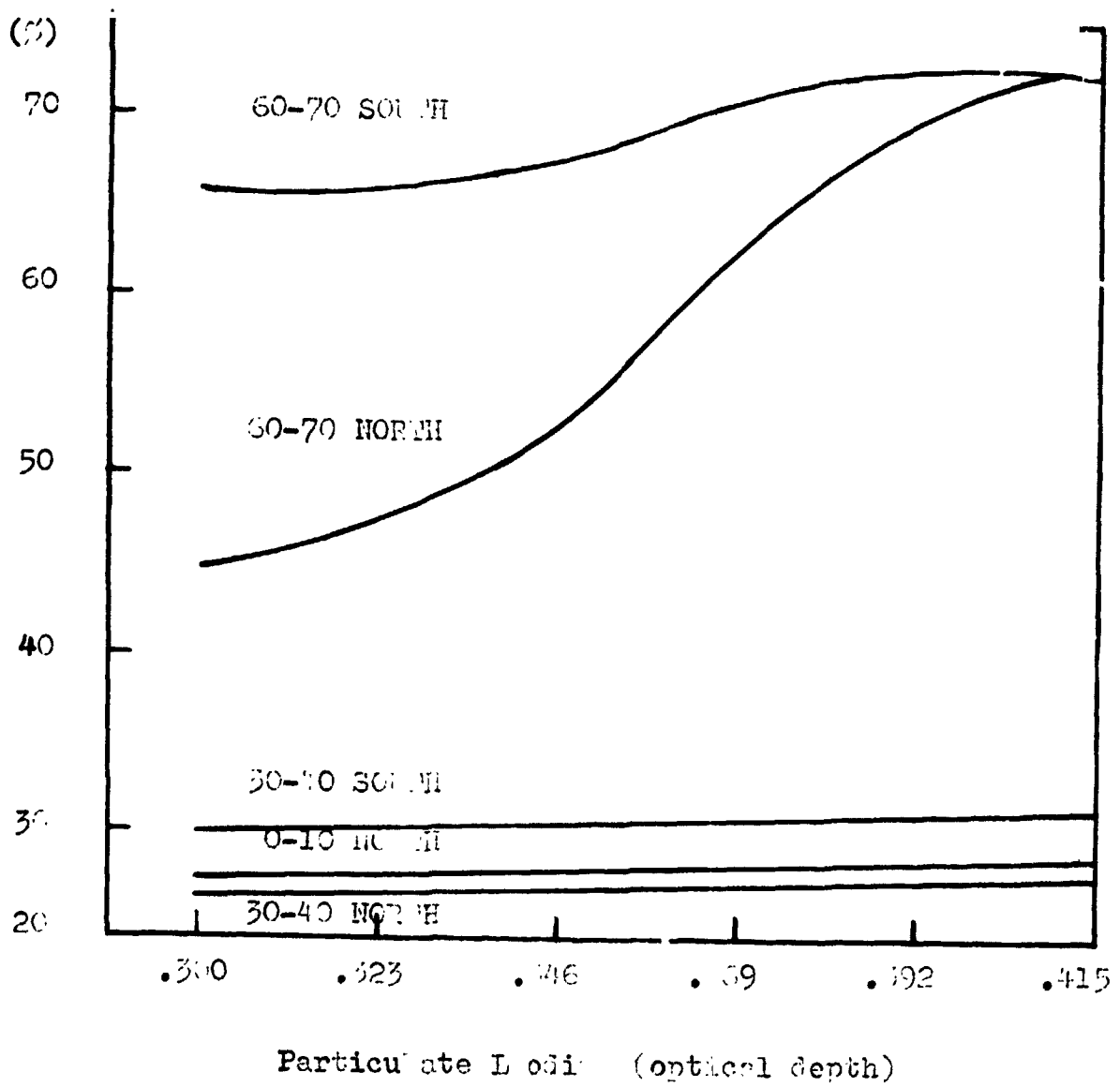


Figure 8. Zonal Albedo for July vs. Particulate Loading

4.2 Variations in Global and Hemispheric Weighted Averages of Earth Radiation Budget Components with Particulate Loading

Variations in global and hemispheric weighted averages for surface temperature and reflected and emitted radiant fluxes with particulate loading for January and July are computed. The results of these computations are found in Appendix C. These results are also plotted in Figures 9 through 14.

Figures 9 and 10 show the variation in average surface temperature with particulate loading. It is found that their functional relationship is non-linearly decreasing. This agrees well with Rasool and Schneider in that the rate of temperature decrease is augmented with increasing aerosol content. This non-linear dependence is due to the backscattering characteristics of the particles. It can be seen by examining the graphs that in order for the average global surface temperature to decrease by 3°C man-made particulate loading must increase by a factor of 4. This increase is seen as an increase in total atmospheric optical depth from 0.300 to 0.369. As previously stated our interest is in the ability to detect a decrease in surface of one-half degree. Examining the graphs reveals that for such a decrease to occur man-made particulate loading must increase by a factor of 2, corresponding to an increase in total atmospheric optical depth from 0.300 to 0.323.

Figures 11 and 12 show the variations in the global and hemispheric weighted averages of short-wave reflected radiant flux with particulate loading for January and July. It is seen that the

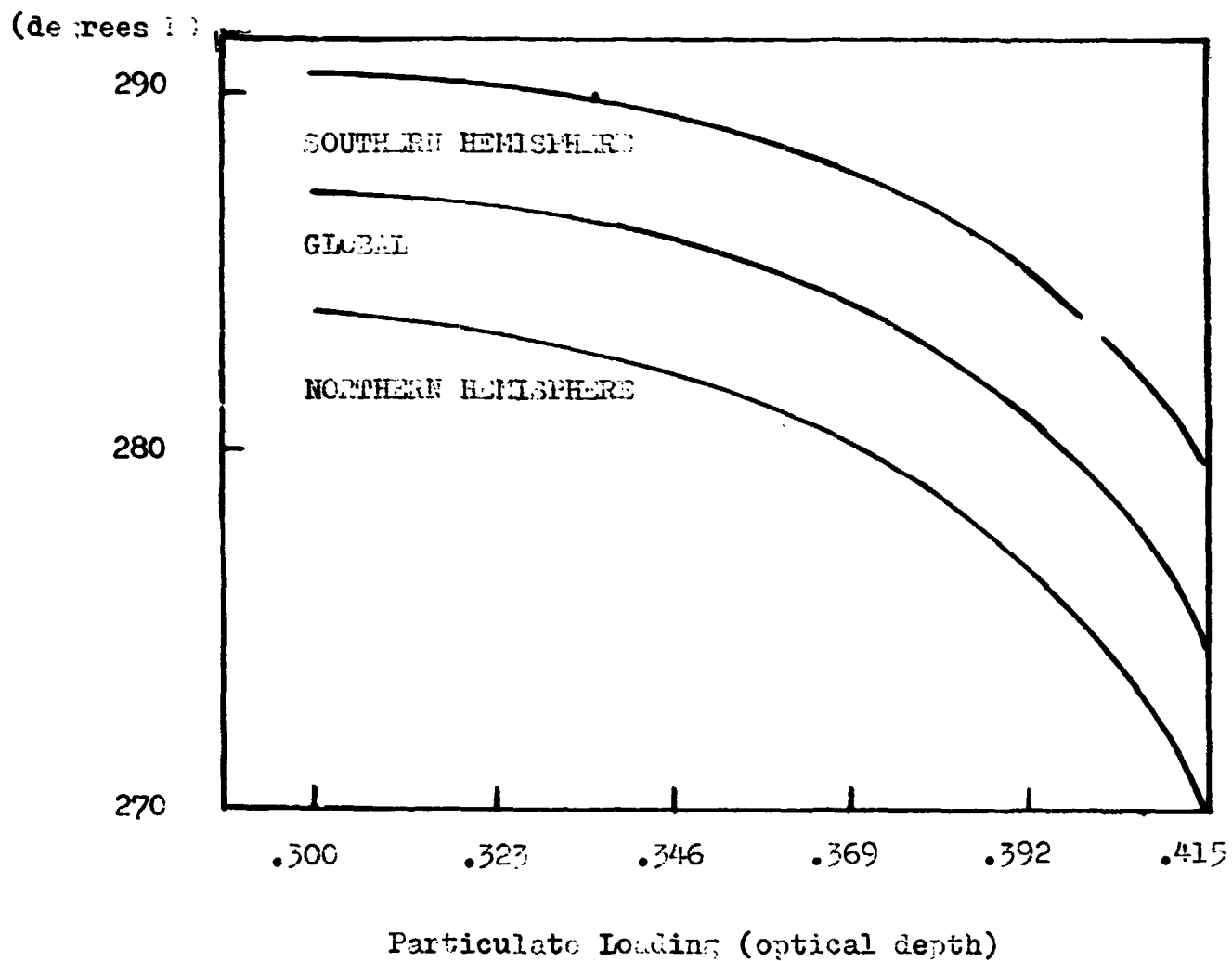


Figure 9. Global and Hemispheric Average Surface Temperatures for January v.s. Particulate Loading

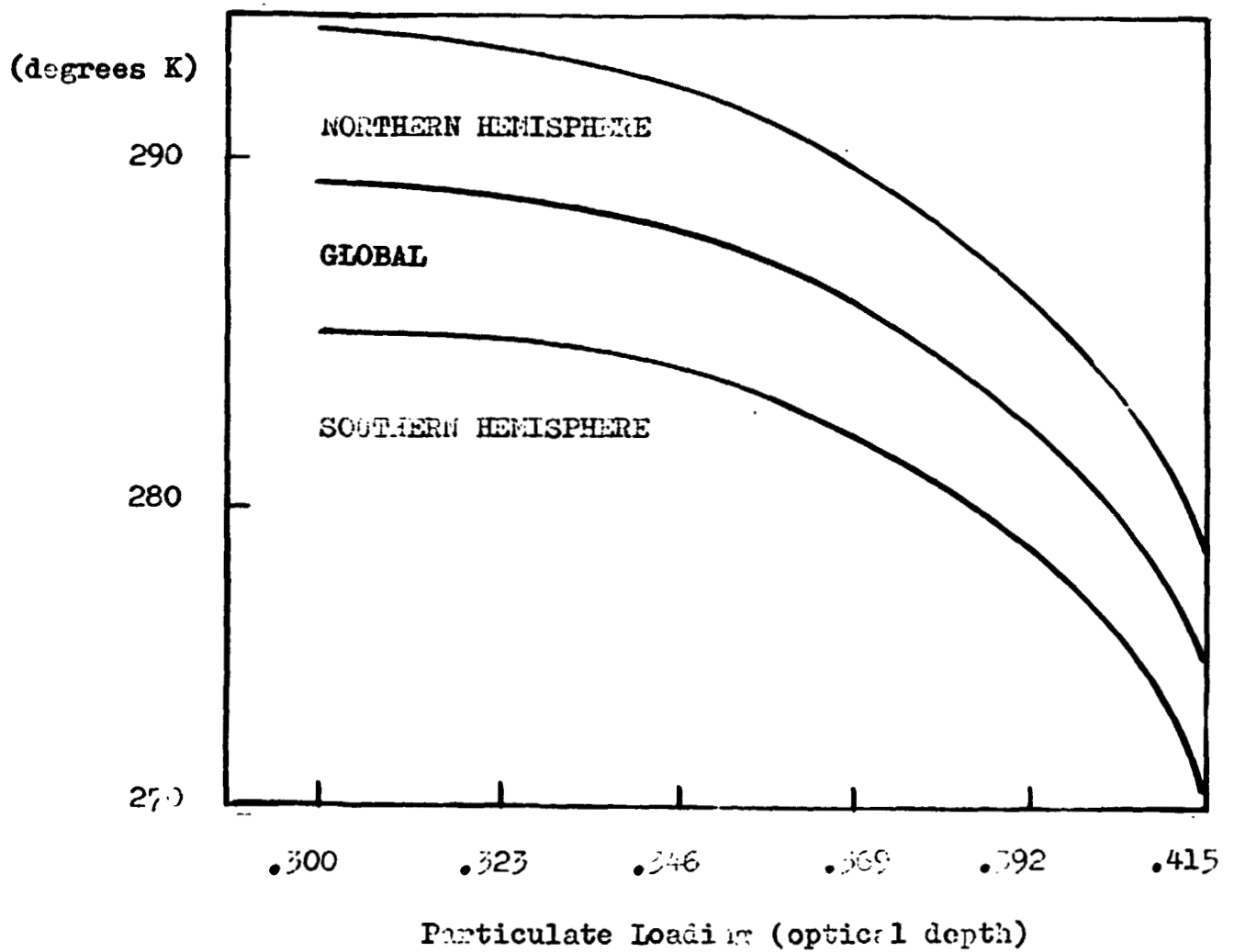


Figure 10. Global and Hemispheric Average Surface Temperatures for July v.s. Particulate Loading

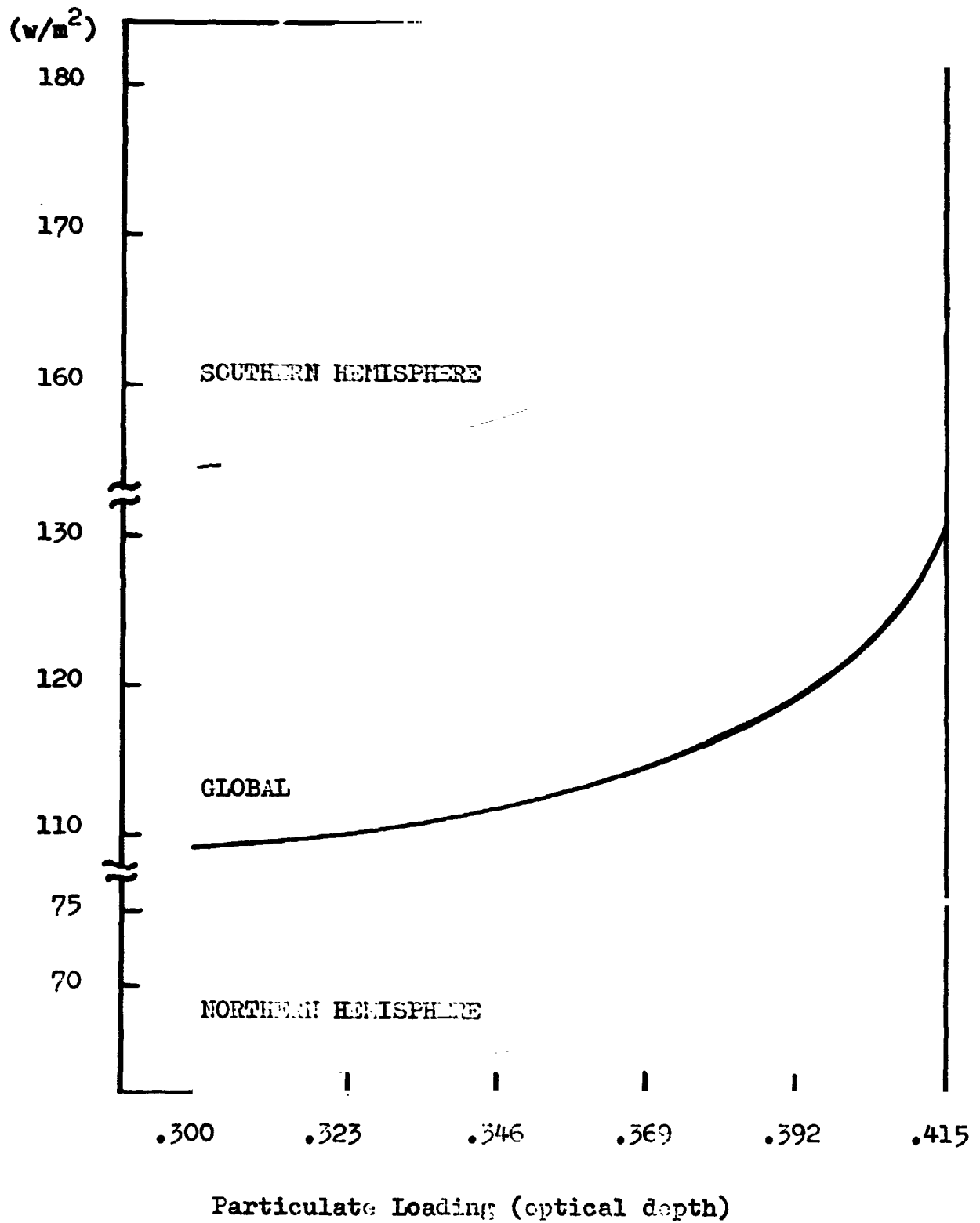


Figure 11. Global and Hemispheric Average Reflected Radiant Flux for January v.s. Particulate Loading

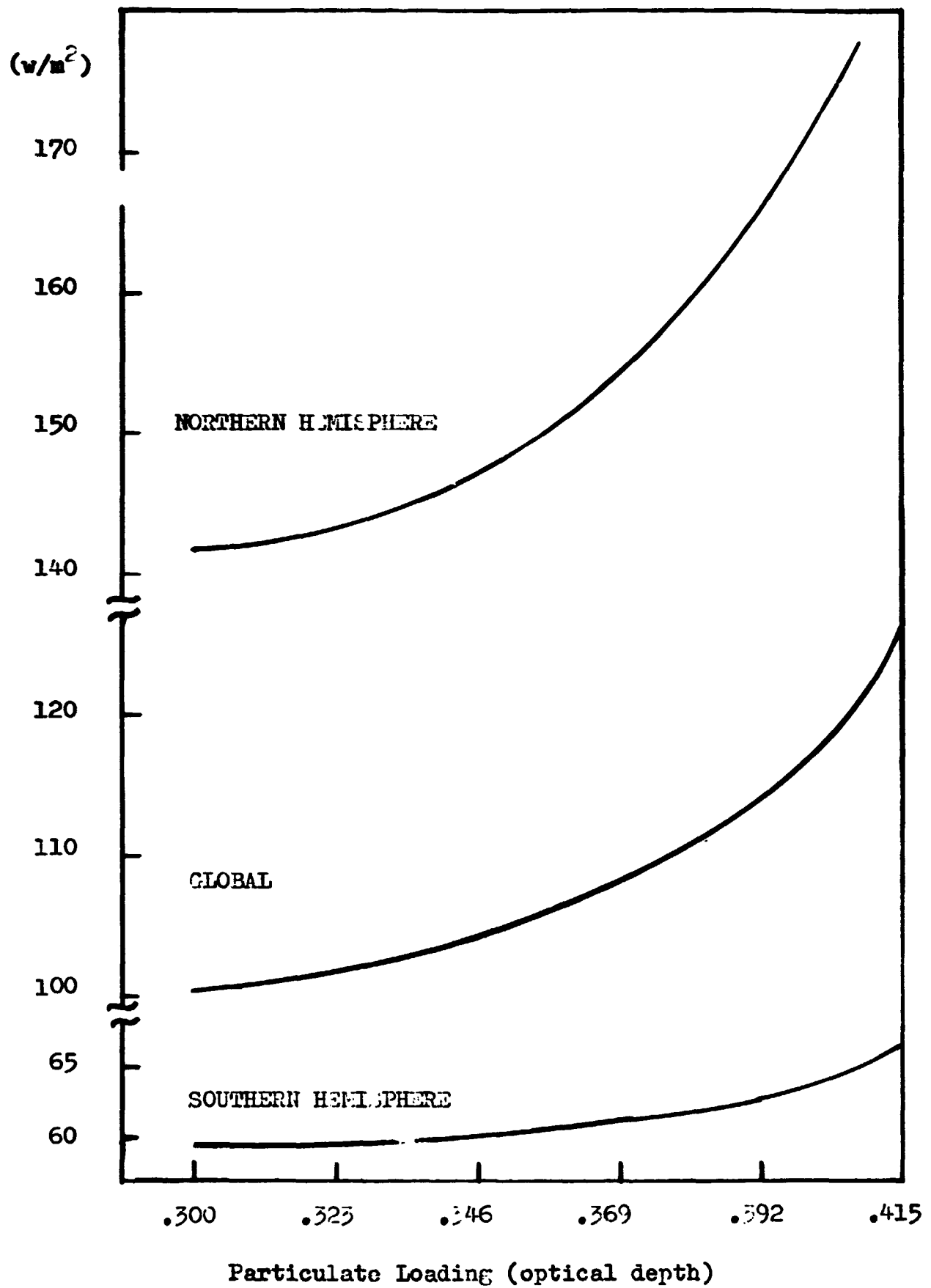


Figure 12. Global and Hemispheric Average Reflected Radiant Flux for July v.s. Particulate Loading

functional relationship between average reflected radiation and particulate loading is non-linearly increasing. Since the incident short-wave reflected radiant flux which is reflected back into space is not available for absorption by the earth's surface there exists an inverse relationship between surface temperature and reflected radiation. As reflected radiant flux changes surface temperature changes in the opposite sense. Therefore, since the functional relationship between surface temperature and particulate loading is non-linearly decreasing the result cited here is reasonable.

Upon examining tables C5 and C6 it is seen that in order to sense a change in particulate optical depth of 0.023, our monitoring instrument must be able, on the average, to sense a change in reflected radiant flux of approximately 1.3 watts/meter².

Figures 13 and 14 show the variations in the global and hemispheric weighted averages of long-wave emitted radiant flux with particulate loading for January and July. Similarly, it is seen that the functional relationship between average emitted radiant flux and particulate loading is non-linearly decreasing. This is due to the direct relationship which exists between emitted radiation on surface temperature. The amount of emitted radiant flux is determined in part by the temperature of the emitting surface. This relationship is known as Stefan-Boltzmann's Law, i.e. emittance is proportional to the fourth power of the temperature of the emitting surface.

Again we wish to be able to detect changes in average emitted radiant flux which corresponds to a change in particulate optical

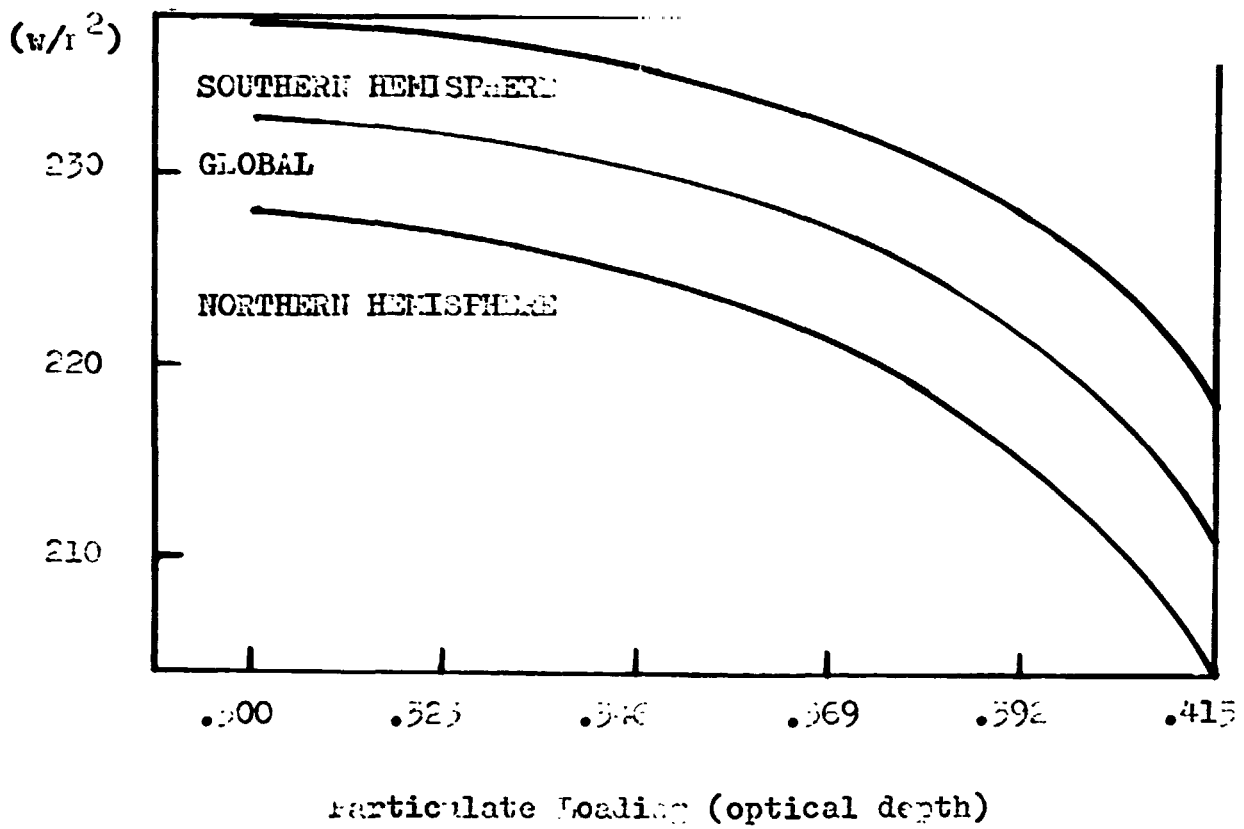


Figure 13. Global and Hemispheric Average Emitted Radiant Flux for January v.s. Particulate Loading

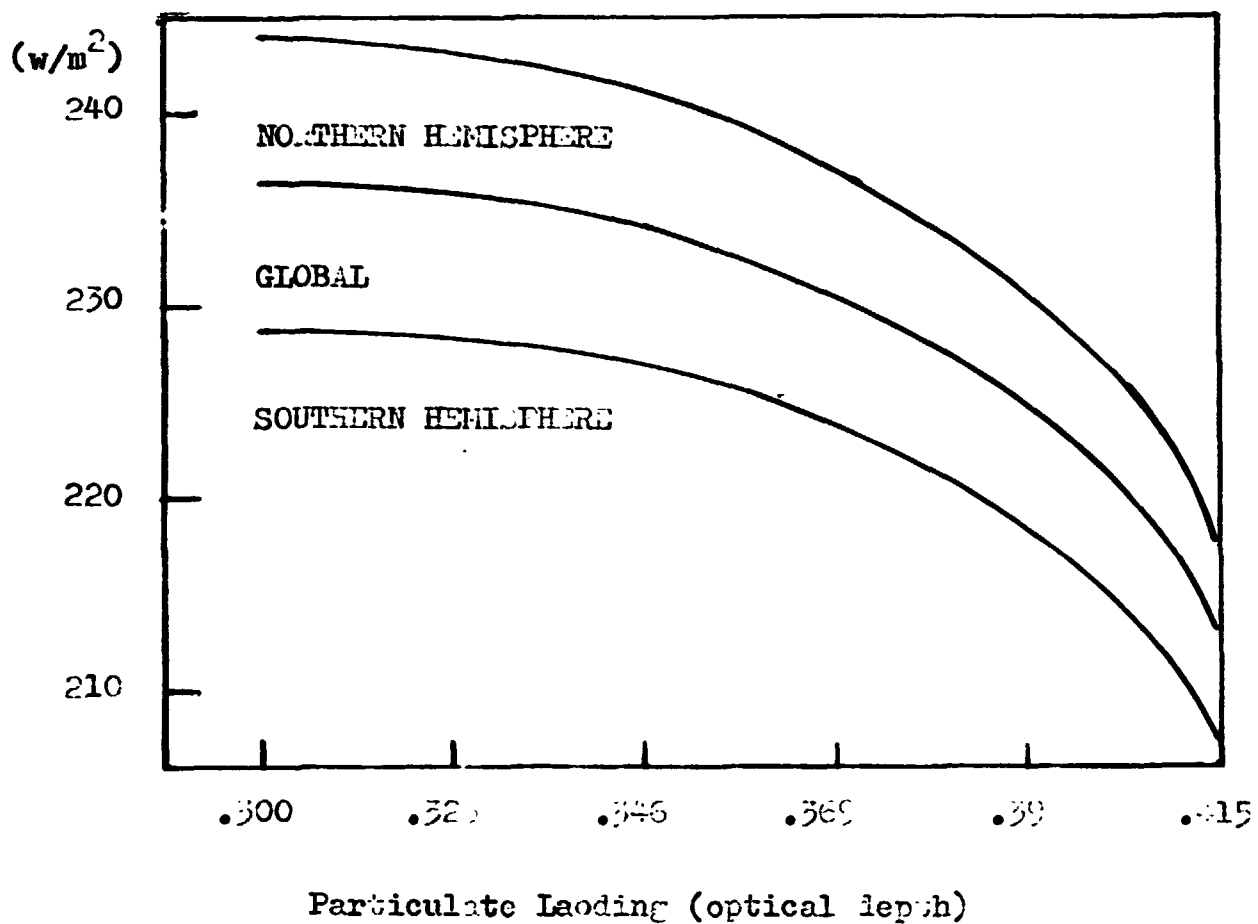


Figure 14. Global and Hemispheric Average Emitted Radiant Flux for July v.s. Particulate Loading

from 0.300 to 0.323. Examining Tables C3 and C4 reveals that in order to sense this increase in optical depth our monitoring instrument must detect a change in emitted radiant flux of approximately 0.8 watts/meter².

4.3 The Feasibility of Monitoring the Effect of Increased Global Particulate Concentrations

A determination of the feasibility of detecting changes in the components of the earth's radiation budget which correspond to a particulate loading increase of 0.023 is performed. In order to determine the feasibility of detecting such changes in the earth's radiation budget it is necessary to compute the changes in equilibrium temperature of the instrument with particulate loading (see approach). The instrument considered is a spherical detector having an emissivity equal to unity (black sphere). The results of these computations are given in the tables below. The global weighted averages for W_e and W_r were used in equations (5) and (6).

Particulate Loading	.300	.323	ΔT	.346	ΔT	.369	ΔT
Day	300.1	300.2	.1	300.3	.2	300.4	.3
Night	182.6	182.4	-.2	182.1	-.5	181.4	-1.2

TABLE 1: Change in Equilibrium Temperature of a Black Sphere as a Function of Particulate Loading for January.

Particulate Loading	.300	.323	ΔT	.346	ΔT	.369	ΔT
Day	299.5	299.6	.1	299.7	.2	299.8	.3
Night	183.3	183.1	-.2	182.8	-.5	182.0	-1.3

TABLE 2: The Zonal Variation of Net-Radiation with Particulate Loading for January

It is seen that day time measurements are much less sensitive to changes in particulate loading than are night time measurements. This is due to the fact that as W_r increases with increased particulate loading W_e decreases an amount such that the resultant change to be sensed by the instrument is nearly canceled. It is seen that a sensitivity of one part in 3000 is needed in order to sense a change in optical depth of 0.023. Therefore, by using a black sphere as the monitoring instrument all daytime measurements may be in the noise of the instrument. If one wishes to use daytime measurements a spherical satellite is needed whose optical characteristics are more sensitive to either W_e or W_r radiant fluxes. For example, an aluminum sphere is 3 to 4 times more sensitive to W_r than is the black sphere. Similarly, white optical characteristics are such that they reflect in part W_r and absorbs W_e in a manner similar to a black sphere.

Examining tables 1 and 2 (black sphere measurements) reveals that in order to be able to sense a change in average surface temperature of one-half degree or an increase in global atmospheric particulate concentrations of 0.023 a satellite monitoring system is needed which can sense a change in its equilibrium temperature of one part per thousand. Such measuring precision can be accomplished at night since there is no reflected radiant flux at this time and therefore changes occurring in the emitted radiation can be sensed by the instrument.

House and Sweet have proposed to AAFE a long term zonal energy budget experiment employing a satellite network which is ideal for the particulate monitoring system described. In the proposal they report an ability to sense changes in the order of one part per thousand. Such precision would be adequate to monitor the effect on climate of increases in global particulates.

V. CONCLUSIONS

Using data, which were generated from a global climate model developed by Sellers, it was possible to determine the feasibility of monitoring the effects of increased global particulate concentrations through the use of existing satellite technology. It was determined that earth radiation budget measurements performed at night by a fleet of proposed black spherical satellites (House and Sweet) are accurate enough to sense a change in global particulate concentrations corresponding to a decrease in average global surface temperature of 0.5°C .

Daytime measurements were found to be of use only if satellites, whose surfaces optically discriminate between either W_e or W_r , are used. It was pointed out that an aluminum or white satellite sphere could be used for the purpose of daytime measurements. It was also found that variations in the global and hemispheric weighted averages of surface temperature, reflected radiant flux and emitted radiant flux are non-linear functions of particulate loading.

Since Sellers' model was used as the basis of the sensitivity calculations, the results can only be as good as the assumptions used in the model. According to Sellers, "Although the model is reasonably complete, in that most of the important atmosphere-land-ocean interactions are included, there is much room for improvement of the various parameterizations." Therefore, these results should only be used to indicate the possibility of using such a technique for global

particulate concentration measurements.

As a follow-up and or check of the validity of these results one could, with a complete record of spacial and temporal variation in albedo, attempt to correlate incidences of high particulate loading (e.g. volcanic erruptions with albedo change.)

APPENDIX A

Zonal Variations in Solar Constant with
Month of Year and Zonal Variation in
Net Radiation with Particulate Loading

In this section is given, in tabular form, the data which was received from Dr. Sellers upon written request. These data include:

- 1) the variation in solar constant with latitude for the twelve months of the year; (one month = 30.4375 days);
- 2) the variation in net radiation average surface temperature and albedo with particulate loading for each ten degree latitude zone for January and July.

These data were provided in units of kly/mo & kly respectively. It was found necessary, for reasons of comparison, to convert from kly to watts/m². Therefore, the data reported in this Appendix are in units of w/m².

TABLE A1: The Variation of Incident Solar Radiant Flux with Latitude for Each Month (H_0 in watts/m²/mo.)

Latitude Zone	Jan	Feb	March	April	May	June	July	Aug	Sep	Oct	Nov	Dec
90-80N	0.00	0.00	42.98	232.4	436.1	526.9	487.1	323.1	105.1	6.367	0.00	0.00
80-70N	0.00	15.92	103.5	254.3	423.4	512.5	471.2	324.7	159.2	41.39	1.592	0.00
70-60N	19.10	68.45	171.9	305.6	425.0	487.1	460.0	355.0	222.8	106.6	31.84	9.551
60-50N	76.40	138.5	240.4	353.4	445.7	488.7	468.0	391.6	284.9	176.7	95.51	58.90
50-40N	146.4	206.9	300.9	394.8	464.8	493.4	479.1	421.8	337.5	243.5	165.5	128.9
40-30N	218.1	273.8	353.4	425.0	472.7	491.9	480.7	442.5	382.0	305.6	235.6	200.6
30-20N	288.1	332.7	396.3	442.5	469.6	477.5	472.8	453.7	413.9	356.5	302.4	272.2
20-10N	350.2	383.6	425.0	448.9	455.2	453.7	452.1	450.5	434.5	401.1	359.7	337.5
10-0N	404.3	423.4	444.1	442.5	428.2	417.0	420.2	433.0	440.9	431.4	410.7	394.8
0-10S	448.9	450.5	447.3	421.8	390.0	370.9	378.8	402.7	434.5	450.5	448.9	445.7
10-20S	480.7	464.8	439.3	388.4	342.2	316.8	326.3	366.1	415.4	453.7	475.9	482.3
20-30S	501.4	466.4	415.4	343.8	284.9	254.7	267.4	315.2	382.0	447.3	490.3	509.4
30-40S	507.8	453.7	380.4	292.9	222.8	187.8	202.2	257.9	340.6	423.4	491.9	520.5
40-50S	506.2	429.8	334.3	230.8	154.4	119.4	132.1	194.2	286.5	391.6	480.7	523.7
50-60S	490.3	396.3	280.1	164.0	87.54	54.12	68.45	125.7	226.0	348.6	460.0	517.3
60-70S	479.1	355.0	214.9	95.50	28.65	7.959	15.92	60.49	157.6	296.1	436.1	515.7
70-80S	490.3	320.0	145.0	31.83	1.592	0.00	0.00	11.14	89.14	243.5	433.0	54.12
80-90S	504.6	213.6	70.73	3.184	0.00	0.00	0.00	0.00	31.84	233.3	445.7	557.1

TABLE A2: The Zonal Variation of Net-Radiation with Particulate Loading for January (Q_n in watts/m²)

Latitude Zone	Particulate Loading					
	.300	.323	.346	.369	.392	.415
90-80N	-163.0	-161.6	-158.7	-154.2	-147.1	-135.1
80-70N	-169.9	-167.8	-165.1	-161.2	154.4	-151.5
70-60N	-177.3	-175.7	-172.5	-168.6	-160.1	-147.6
60-50N	-160.1	-160.1	-160.3	-160.3	-156.2	-146.0
50-40N	-117.6	-117.3	-118.3	-120.9	-124.6	-133.2
40-30N	-82.00	-81.34	-80.23	-77.04	-71.63	-77.04
30-20N	-44.41	-44.10	-43.46	-40.75	-35.97	-25.47
20-10N	-0.478	-0.478	0.000	2.228	6.367	15.60
10-0N	36.93	36.93	37.25	39.32	43.30	52.05
0-10S	64.63	64.47	64.63	66.70	70.67	79.27
10-20S	87.07	86.59	86.75	88.66	92.32	100.9
20-30S	100.6	100.1	100.1	101.9	105.5	114.3
30-40S	114.3	113.7	113.7	115.6	119.4	128.5
40-50S	114.4	113.8	114.0	116.2	120.3	81.34
50-60S	98.85	96.78	91.05	74.49	42.34	-15.60
60-70S	24.83	23.08	16.71	0.159	-25.79	-49.98
70-80S	-49.50	-49.19	-51.26	-59.37	-54.60	-45.52
80-90S	-54.76	-54.12	-52.53	-49.34	-44.89	-36.29

TABLE A3: The Zonal Variation of Net-Radiation with Particulate Loading for July (Q_n in watts/m²)

Latitude Zone	Particulate Loading					
	.300	.323	.346	.369	.392	.415
90-80N	-20.37	-30.08	-47.12	-50.62	-43.14	-31.34
80-70N	7.004	-2.228	-14.64	-43.30	-57.46	-44.25
70-60N	29.75	19.10	1.592	-37.25	-58.90	-56.35
60-50N	76.09	76.72	78.31	58.90	5.730	-51.10
50-40N	83.89	84.05	85.16	88.98	95.51	19.58
40-30N	89.30	89.14	89.62	92.64	98.05	110.2
30-20N	73.22	73.06	73.38	75.93	80.86	91.37
20-10N	58.10	57.94	58.42	60.65	65.10	74.34
10-0N	43.30	43.14	43.46	45.68	49.82	58.58
0-10S	17.67	17.35	17.67	19.74	23.88	32.63
10-20S	-15.92	-16.24	-15.92	-13.85	-0.710	-0.637
20-30S	-58.74	-58.74	-58.26	-55.87	-51.57	-41.86
30-40S	-95.51	-95.35	-94.71	-92.00	-87.39	-77.20
40-50S	-13.18	-131.6	-130.7	-12.75	-125.1	-131.5
50-60S	-162.4	-162.4	-162.0	-16.11	-160.4	-153.6
60-70S	-178.8	-178.4	-177.2	-17.30	-166.7	-154.4
70-80S	-171.3	-171.0	-169.5	-16.52	-159.0	-147.4
80-90S	-156.0	-155.7	-154.6	-15.06	-144.5	-133.5

TABLE A4: The Zonal Variation of Average Surface Temperature with Particulate Loading for January (Degrees K)

Latitude Zone	Particulate Loading					
	.300	.323	.346	.369	.392	.415
90-80N	245.1	243.6	241.6	238.7	233.7	224.9
80-70N	251.1	249.7	247.8	245.1	239.8	230.9
70-60N	259.8	258.7	257.1	253.7	247.8	238.5
60-50N	268.9	268.1	266.9	264.0	259.1	248.7
50-40N	277.9	277.3	276.3	274.0	270.3	262.0
40-30N	286.4	285.8	285.0	283.1	279.9	273.3
30-30N	292.2	291.7	290.9	289.3	286.4	280.6
20-10N	296.0	295.5	294.8	293.2	290.5	285.2
10-0N	298.1	297.6	296.9	295.4	292.7	287.5
0-10S	299.0	298.5	297.8	296.2	293.5	288.3
10-20S	299.4	299.0	298.3	296.8	294.3	289.2
20-30S	297.9	297.6	297.0	295.4	292.9	287.8
30-40S	293.2	292.9	292.2	290.6	288.0	282.5
40-50S	286.4	286.2	285.5	283.7	280.9	274.7
50-60S	278.9	278.7	277.9	276.0	273.0	266.8
60-70S	271.8	271.6	270.9	269.1	266.3	260.4
70-80S	266.7	266.6	265.8	263.9	261.2	255.6
80-90S	262.9	262.7	262.1	260.3	257.7	252.2

TABLE A5: The Zonal Variation of Average Surface Temperature with Particulate Loading for July (Degrees K)

Latitude Zone	Particulate Loading					
	.300	.323	.346	.369	.392	.415
90-80N	268.0	267.3	266.0	262.8	257.7	249.3
80-70N	272.9	271.9	270.4	267.0	261.8	253.0
70-60N	280.2	279.1	277.3	273.1	267.4	258.0
60-50N	286.5	285.7	284.4	280.9	275.3	265.0
50-40N	292.3	291.6	290.5	288.0	283.6	274.7
40-30N	296.7	296.2	295.3	293.2	289.8	282.9
30-20N	299.4	298.8	298.1	296.2	293.1	287.1
20-10N	299.3	298.9	298.2	296.5	293.6	288.1
10-0N	298.8	298.4	297.7	296.0	293.3	288.1
0-10S	298.1	297.7	297.1	295.5	292.9	287.7
10-20S	296.6	296.2	295.7	294.1	291.6	286.4
20-30S	293.2	292.9	292.3	290.8	288.2	282.8
30-40S	287.6	287.4	286.8	285.1	282.3	276.3
40-50S	279.7	279.6	278.9	276.9	273.6	265.3
50-60S	270.6	270.4	269.6	266.9	262.6	253.0
60-70S	260.8	260.6	259.7	256.5	252.1	243.3
70-80S	252.4	252.2	251.3	248.5	244.1	235.7
80-90S	246.4	246.2	245.3	242.5	238.2	230.0

TABLE A6: The Zonal Variation of Albedo with Particulate Loading for January (A in%)

Latitude Zone	Particulate Loading					
	.300	.323	.346	.369	.392	.415
90-80N	74.5	74.3	74.2	74.0	73.8	73.6
80-70N	73.0	72.9	72.8	72.7	72.6	72.5
70-60N	67.2	67.7	68.6	71.1	72.9	72.8
60-50N	48.7	50.6	53.6	60.0	65.4	72.8
50-40N	32.8	33.4	35.4	39.9	47.0	62.9
40-30N	29.4	29.6	29.8	30.0	30.2	38.5
30-20N	27.9	28.1	28.4	28.6	28.8	29.1
20-10N	25.9	26.1	26.4	26.7	26.9	27.2
10-0N	26.0	26.2	26.5	26.7	27.0	27.2
0-10S	26.7	26.9	27.2	27.4	27.6	27.9
10-20S	26.5	26.8	27.0	27.3	27.5	27.7
20-30S	26.9	27.2	27.4	27.7	27.9	28.1
30-40S	27.2	27.5	27.7	28.0	28.2	28.4
40-50S	30.3	30.5	30.7	30.9	31.1	41.2
50-60S	34.7	35.2	36.6	40.8	47.9	62.9
60-70S	51.9	52.3	53.9	58.1	64.6	71.6
70-80S	70.1	70.1	70.8	73.1	73.0	72.9
80-90S	74.7	74.6	74.5	74.4	74.2	74.1

TABLE A7: The Zonal Variation of Albedo as a Function of Particulate Loading for July (A in %)

Latitude Zone	Particulate Loading					
	.300	.323	.346	.369	.392	.415
90-80N	63.6	65.9	69.9	71.6	71.5	71.5
80-70N	54.3	56.6	59.9	67.3	72.2	72.1
70-60N	44.9	47.7	52.4	62.7	69.7	72.4
60-50N	33.1	33.3	33.5	39.1	53.0	69.4
50-40N	30.2	30.4	30.6	30.8	31.0	51.0
40-30N	26.5	26.7	26.9	27.2	27.4	27.7
30-20N	27.5	27.8	28.0	28.3	28.5	28.7
20-10N	29.0	29.2	29.4	29.6	29.8	30.0
10-0N	27.4	27.6	27.9	28.1	28.3	28.5
0-10S	26.1	26.4	26.6	26.9	27.1	27.4
10-20S	25.0	25.3	25.5	25.8	26.1	26.3
20-30S	27.9	28.1	28.4	28.6	28.8	29.1
30-40S	30.0	30.2	30.5	20.7	30.9	31.3
40-50S	35.2	35.3	35.5	35.7	38.1	53.8
50-60S	44.0	44.5	46.1	51.3	60.6	72.3
60-70S	65.5	65.8	67.1	71.0	72.5	72.3
70-80S	74.2	74.0	73.9	73.8	73.6	73.5
80-90S	75.4	75.3	75.1	75.0	74.9	74.7

APPENDIX B

Zonal Variations of Emitted and Reflected Radiant Fluxes with Particulate Loading

By operating on the data listed in Appendix A with equations (1) and (2) it was possible to generate the zonal variation in emitted long-wave radiation (W_e) and reflected short-wave radiation (W_r) as a function of particulate loading.

The results from these calculations are reported below.

TABLE B1: The Zonal Variation of Emitted Radiant Flux with Particulate Loading for January (W_e in watts/m²)

Latitude Zone	Particulate Loading					
	.300	.323	.346	.369	.392	.415
90-80N	163.0	161.6	158.7	154.2	147.1	135.1
80-70N	169.8	167.8	165.1	161.2	154.4	151.5
70-60N	183.4	181.7	178.4	173.9	165.2	152.6
60-50N	198.2	196.7	194.7	189.9	181.8	166.1
50-40N	213.1	211.9	210.0	206.2	199.9	185.9
40-30N	231.3	230.3	228.7	225.1	219.3	207.1
30-20N	245.9	245.0	243.6	240.3	235.0	223.6
20-10N	252.2	251.5	250.0	246.8	241.9	231.7
10-0N	253.3	252.5	251.0	248.1	243.0	233.5
0-10S	254.5	253.8	252.4	249.4	244.6	234.7
10-20S	255.7	254.7	253.6	250.3	245.7	236.1
20-30S	254.9	253.9	253.0	249.8	245.1	235.4
30-40S	244.3	243.4	242.5	239.1	234.3	224.2
40-50S	227.8	227.4	226.3	223.1	218.0	207.4
50-60S	211.7	211.4	210.5	207.0	205.4	192.0
60-70S	198.7	198.6	197.5	194.6	190.3	182.0
70-80S	191.7	191.4	190.1	187.3	183.0	174.4
80-90S	178.6	178.4	177.3	174.6	171.2	163.1

TABLE B2: The Zonal Variation in Emitted Radiant Flux with Particulate Loading for July (W_e in watts/m²)

Latitude Zone	Particulate Loading					
	.300	.323	.346	.369	.392	.415
90-80N	192.4	191.2	189.3	184.8	177.8	166.5
80-70N	201.9	200.6	197.9	192.7	184.5	171.8
70-60N	216.1	214.3	210.8	203.7	194.1	179.5
60-50N	227.6	226.1	223.6	217.6	207.6	190.0
50-40N	240.5	239.4	237.4	232.6	225.2	208.1
40-30N	253.4	252.7	251.2	246.8	240.5	227.0
30-20N	259.2	258.0	256.8	252.9	247.0	235.6
20-10N	253.2	252.5	251.2	248.1	242.7	232.6
10-0N	252.6	252.0	250.4	247.4	242.4	232.9
0-10S	253.9	252.1	252.1	248.9	244.0	234.2
10-20S	253.3	252.7	251.7	248.7	243.6	233.9
20-30S	245.7	245.2	244.0	241.1	236.3	225.8
30-40S	232.7	232.2	231.0	227.9	222.9	211.9
40-50S	214.8	214.6	213.3	209.9	204.4	190.7
50-60S	199.5	199.2	197.8	193.4	186.6	172.0
60-70S	184.1	183.6	182.2	177.5	170.9	158.7
70-80S	171.3	171.0	169.5	165.2	159.0	147.4
80-90S	156.0	155.7	154.6	150.6	144.5	133.5

TABLE B3: The Zonal Variation in Reflected Radiant Flux with Particulate Loading for January (W_r in watts/m²)

Latitude Zone	Particulate Loading					
	.300	.323	.346	.369	.392	.415
90-80N	0.000	0.000	0.000	0.000	0.000	0.000
80-70N	0.000	0.000	0.000	0.000	0.000	0.000
70-60N	12.46	12.54	12.71	13.17	13.51	13.49
60-50N	36.09	37.50	39.72	44.47	48.47	53.95
50-40N	46.59	47.44	50.29	56.68	66.76	89.35
40-30N	62.19	62.61	63.04	63.46	63.88	81.44
30-20N	77.97	78.53	79.37	79.93	80.49	81.32
20-10N	87.97	88.66	89.68	90.70	91.37	92.39
10-0N	102.0	102.8	103.9	104.7	105.9	106.7
0-10S	116.3	117.1	118.4	119.3	120.2	121.5
10-20S	123.6	125.0	125.9	127.3	128.2	129.2
20-30S	130.8	132.3	133.3	134.7	135.7	136.7
30-40S	134.0	135.4	136.4	137.9	138.9	139.9
40-50S	148.8	149.8	150.7	151.7	152.7	202.3
50-60S	165.0	167.4	174.1	194.0	227.8	299.1
60-70S	241.2	243.1	255.5	270.0	300.2	332.8
70-80S	333.4	333.4	336.7	347.6	347.2	346.7
80-90S	365.6	365.1	364.6	364.2	363.2	362.7

TABLE B4: The Zonal Variation in Radiant Flux with Loading for July (W_p in watts/m²)

Latitude Zone	Particulate Loading					
	.300	.323	.346	.369	.392	.415
90-80N	300.5	311.4	330.3	338.3	337.8	337.8
80-70N	248.2	258.7	273.8	307.6	330.0	329.5
70-60N	200.4	212.8	233.8	279.8	311.0	323.1
60-50N	150.3	151.2	152.1	177.5	240.6	315.0
50-40N	140.4	141.3	142.2	143.1	144.1	237.0
40-30N	123.6	124.5	125.4	126.8	127.8	129.2
30-20N	126.1	127.5	128.4	129.8	130.7	131.6
20-10N	127.2	128.0	128.9	129.8	130.7	131.5
10-0N	111.7	112.5	113.7	11.45	115.4	116.2
0-10S	95.91	97.01	97.94	98.85	99.59	100.7
10-20S	19.13	80.08	80.71	81.66	82.61	83.25
20-30S	72.37	72.89	73.67	74.18	74.71	75.48
30-40S	58.82	59.22	59.81	60.20	60.59	61.38
40-50S	45.11	45.24	45.49	45.75	48.83	68.95
50-60S	29.21	25.55	30.61	34.06	40.23	48.00
60-70S	10.11	10.16	10.36	10.96	11.19	11.16
70-80S	0.000	0.000	0.000	0.000	0.000	0.000
80-90S	0.000	0.000	0.000	0.000	0.000	0.000

APPENDIX C

Variations in Global and Hemispheric Weighted Averages of Surface Temperature and Emitted and Reflected Radiant Fluxes with Particulate Loading

Using the data from Appendices A and B, global and hemispheric weighted averages for surface temperature, emitted radiation and reflected radiation as a function of particulate loading for January and July were generated using equations (3) and (4).

These data are reported below.

TABLE C1: Global and Hemispheric Weighted Averages of Surface Temperature with Particulate Loading for January (Degrees K)

Particulate Loading	Northern Hemisphere	Southern Hemisphere	Global
.300	284.0	290.5	287.2
.323	283.3	290.2	286.7
.346	282.4	289.5	285.9
.369	280.3	287.8	284.1
.392	276.8	285.1	281.0
.415	269.8	279.6	274.7

TABLE C2: Global and Hemispheric Weighted Averages of Surface Temperature with Particulate Loading for July (Degrees K)

Particulate Loading	Northern Hemisphere	Southern Hemisphere	Global
.300	293.6	285.0	289.3
.323	293.0	284.7	288.9
.346	292.1	284.0	288.0
.369	289.7	282.0	285.9
.392	285.9	279.0	282.5
.415	278.9	272.3	275.6

TABLE C3: Global and Hemispheric Weighted Averages of Emitted Radiant Flux with Particulate Loading for January (W_e in w/m^2)

Particulate Loading	Northern Hemisphere	Southern Hemisphere	Global
.300	228.0	237.6	232.8
.323	227.0	237.0	232.0
.346	225.1	235.8	230.5
.369	221.6	232.7	227.1
.392	215.5	228.3	221.9
.415	204.1	218.2	211.1

TABLE C4: Global and Hemispheric Weighted Averages of Emitted Radiant Flux with Particulate Loading for July (W_e in w/m^2)

Particulate Loading	Northern Hemisphere	Southern Hemisphere	Global
.300	244.0	228.9	236.4
.323	242.9	228.3	235.6
.346	241.1	227.2	234.2
.369	236.8	223.7	230.3
.392	227.1	218.3	222.2
.415	217.4	207.0	212.2

TABLE C5: Global and Hemispheric Weighted Averages of Reflected Radiant Flux with Particulate Loading for January (W_r in w/m^2)

Particulate Loading	Northern Hemisphere	Southern Hemisphere	Global
.300	63.96	154.0	109.0
.323	64.62	155.4	110.0
.346	65.77	157.5	111.6
.369	67.52	162.4	115.0
.392	69.66	168.7	119.2
.415	75.93	185.0	130.5

TABLE C6: Global and Hemispheric Weighted Averages of Reflected Radiant Flux with Particulate Loading for July (W_r in w/m^2)

Particulate Loading	Northern Hemisphere	Southern Hemisphere	Global
.300	141.3	59.02	100.1
.323	143.7	59.56	101.6
.346	147.0	60.15	103.6
.369	155.4	61.06	108.2
.392	165.7	62.50	114.1
.415	186.1	66.27	126.2

APPENDIX D

Computer Program

The following computer program was used to generate the data which appears in Appendices B and C. It also accomplishes the conversion of units from kLys to w/m^2 . The program is written in standard FORTRAN IV coding.

```

DIMENSION QS(18,12),RNJA(18,6),RNJU(18,6),TOJA(18,6),TOJU(18,6),
1ALHJA(18,6),ALBJU(18,6),ERJA(18,6),ERJU(18,6),REFJA(18,6),
IREFJU(18,6),QSW(18,12),RNJAN(18,6),RNJUN(18,6),
1TOJAK(18,6),TOJUK(18,6)
READ(5,100)((QS(I,J),I=1,18),J=1,12),((RNJA(I,J),I=1,18),J=1,6),
1((RNJU(I,J),I=1,18),J=1,6),((TOJA(I,J),I=1,18),J=1,6),
1((TOJU(I,J),I=1,18),J=1,6),((ALHJA(I,J),I=1,18),J=1,6),
1((ALBJU(I,J),I=1,18),J=1,6)
WRITE(6,99)QS
WRITE(6,100)RNJA,RNJU,TOJA,TOJU,ALHJA,ALBJU
99 FORMAT(12F10.3)
100 FORMAT(6F10.3)
C JA & JU STAND FOR JANUARY & JULY RESPECTIVELY, ER STANDS FOR EMITTED
C RADIATION, REF REFERS TO THE REFLECTED RADIATION.
CF=4.186E+07/(86400.*30.4375)
DO 10 J=1,12
DO 10 I=1,18
10 QSW(I,J)=QS(I,J)*CF
WRITE(6,101)
101 FORMAT(" ",T50,"QSW(WATTS/METER**2)")
DO 11 I=1,9
K=90-(I*10)
L=K+10
11 WRITE(6,102)L,K,(QSW(I,J),J=1,12)
102 FORMAT(" ",I2,"=",I2,"N",12F10.3)
DO 12 I=10,18
K=(I-10)*10
L=K+10
12 WRITE(6,103)K,L,(QSW(I,J),J=1,12)
103 FORMAT(" ",I2,"=",I2,"S",12F10.3)
DO 13 J=1,6
DO 13 I=1,18
13 RNJAN(I,J)=RNJA(I,J)*CF
WRITE(6,104)
104 FORMAT(" ",T30,"RN=JAN (WATTS/METER**2)")
DO 14 I=1,9
K=90-(I*10)
L=K+10
14 WRITE(6,105)L,K,(RNJAN(I,J),J=1,6)
105 FORMAT(" ",I2,"=",I2,"N",6F10.3)
DO 15 I=10,18
K=(I-10)*10
L=K+10
15 WRITE(6,106)K,L,(RNJAN(I,J),J=1,6)
106 FORMAT(" ",I2,"=",I2,"S",6F10.3)
DO 16 J=1,6
DO 16 I=1,18
16 RNJUN(I,J)=RNJU(I,J)*CF
WRITE(6,107)
107 FORMAT(" ",T30,"RN=JULY (WATTS/METER**2)")
DO 17 I=1,9
K=90-(I*10)
L=K+10
17 WRITE(6,108)L,K,(RNJUN(I,J),J=1,6)

```

```

108 FORMAT(" ",I2,"-",I2,"N",6F10.3)
DO 18 I=10,18
K=(I-10)*10
L=K+10
18 WRITE(6,109)K,L,(RNJUN(I,J),J=1,6)
109 FORMAT(" ",I2,"-",I2,"S",6F10.3)
DO 31 J=1,6
DO 31 I=1,18
31 TOJAK(I,J)=TOJA(I,J)+273.0
WRITE(6,130)
130 FORMAT(" ",T30,"TO-JA(DEGREES K)")
DO 32 I=1,9
K=90-(I*10)
L=K+10
32 WRITE(6,131)L,K,(TOJAK(I,J),J=1,6)
131 FORMAT(" ",I2,"-",I2,"N",6F10.3)
DO 33 I=10,18
K=(I-10)*10
L=K+10
33 WRITE(6,132)K,L,(TOJAK(I,J),J=1,6)
132 FORMAT(" ",I2,"-",I2,"S",6F10.3)
DO 34 J=1,6
DO 34 I=1,18
34 TOJUK(I,J)=TOJU(I,J)+273.0
WRITE(6,133)
133 FORMAT(" ",T30,"TO-JU(DEGREES K)")
DO 35 I=1,9
K=90-(I*10)
L=K+10
35 WRITE(6,134)L,K,(TOJUK(I,J),J=1,6)
134 FORMAT(" ",I2,"-",I2,"N",6F10.3)
DO 36 I=10,18
K=(I-10)*10
L=K+10
36 WRITE(6,135)K,L,(TOJUK(I,J),J=1,6)
135 FORMAT(" ",I2,"-",I2,"S",6F10.3)
DO 19 J=1,6
DO 19 I=1,18
19 ERJA(I,J)=(.97*QSW(I,1)*(1.-ALBJA(I,J)))-RNJAN(I,J)
C QSW(I,1) IS THE LATITUDINAL VARIATION OF THE SOLAR CONSTANT IN THE
C MONTH OF JANUARY
WRITE(6,110)
110 FORMAT(" ",T20,"EMITTED RADIATION (JANUARY)")
DO 20 I=1,9
K=90-(I*10)
L=K+10
20 WRITE(6,111)L,K,(ERJA(I,J),J=1,6)
111 FORMAT(" ",I2,"-",I2,"N",6F10.3)
DO 21 I=10,18
K=(I-10)*10
L=K+10
21 WRITE(6,112)K,L,(ERJA(I,J),J=1,6)
112 FORMAT(" ",I2,"-",I2,"S",6F10.3)
DO 22 J=1,6
DO 22 I=1,18
22 ERJU(I,J)=(.97*QSW(I,7)*(1.-ALBJU(I,J)))-RNJUN(I,J)
C QSW(I,7) IS THE LATITUDINAL VARIATION OF THE SOLAR CONSTANT IN THE
C MONTH OF JULY
WRITE(6,113)
113 FORMAT(" ",T20,"EMITTED RADIATION (JULY)")
DO 23 I=1,9
K=90-(I*10)

```

ORIGINAL PAGE IS
OF POOR

```

L=K+10
23 WRITE(6,114)L,K,(EHJU(1,J),J=1,6)
114 FORMAT(" ",12,"-",12,"N",6F10.3)
DO 24 I=10,18
K=(I-10)*10
L=K+10
24 WRITE(6,115)K,L,(EHJU(1,J),J=1,6)
115 FORMAT(" ",12,"-",12,"S",6F10.3)
DO 25 J=1,6
DO 25 I=1,18
25 REFJA(1,J)=.97*QSW(I,1)*ALHJA(1,J)
WRITE(6,116)
116 FORMAT(" ",T20,"REFLECTED RADIATION(JANUARY)")
DO 26 I=1,9
K=90-(I*10)
L=K+10
26 WRITE(6,117)L,K,(REFJA(1,J),J=1,6)
117 FORMAT(" ",12,"-",12,"N",6F10.3)
DO 27 I=10,18
K=(I-10)*10
L=K+10
27 WRITE(6,118)K,L,(REFJA(1,J),J=1,6)
118 FORMAT(" ",12,"-",12,"S",6F10.3)
DO 28 J=1,6
DO 28 I=1,18
28 REFJU(1,J)=.97*QSW(I,7)*ALBJU(1,J)
WRITE(6,119)
119 FORMAT(" ",T20,"REFLECTED RADIATION(JULY)")
DO 29 I=1,9
K=90-(I*10)
L=K+10
29 WRITE(6,120)L,K,(REFJU(1,J),J=1,6)
120 FORMAT(" ",12,"-",12,"N",6F10.3)
DO 30 I=10,18
K=(I-10)*10
L=K+10
30 WRITE(6,121)K,L,(REFJU(1,J),J=1,6)
121 FORMAT(" ",12,"-",12,"S",6F10.3)
C FIND GLOBAL & HEMISPHERICAL WEIGHTED AVERAGES FOR SURFACE TEMP. IN
C JANUARY, SURFACE TEMP. IN JULY, NET RADIATION IN JANUARY &
C JULY, EMITTED RADIATION IN JANUARY & JULY AND REFLECTED RADIATION
C IN JANUARY & JULY
WRITE(6,122)
122 FORMAT(" ",T30,"AVERAGE SURFACE TEMPERATURE FOR JANUARY")
CALL AVER(TOJAK)
WRITE(6,123)
123 FORMAT(" ",T25,"AVERAGE SURFACE TEMPERATURE FOR JULY")
CALL AVER(TOJUK)
WRITE(6,124)
124 FORMAT(" ",T25,"AVERAGE NET RADIATION FOR JANUARY")
CALL AVER(RNJAK)
WRITE(6,125)
125 FORMAT(" ",T25,"AVERAGE NET RADIATION FOR JULY")

CALL AVER(RNJUN)
WRITE(6,126)
126 FORMAT(" ",T25,"AVERAGE EMITTED RADIATION FOR JANUARY")
CALL AVER(ERJA)
WRITE(6,127)
127 FORMAT(" ",T25,"AVERAGE EMITTED RADIATION FOR JULY")
CALL AVER(ERJU)
WRITE(6,128)
128 FORMAT(" ",T25,"AVERAGE REFLECTED RADIATION FOR JANUARY")

```

ORIGINAL PAGE IS
OF POOR QUALITY

```

CALL AVER(REFJA)
WRITE(6,129)
129 FORMAT(" ",T25,"AVERAGE REFLECTED RADIATION FOR JULY")
CALL AVER(REFJU)
STOP
END

```

```

SUBROUTINE AVER (Y)
REAL NORTH
DIMENSION X(18,6),SUMN(6),NORTH(6),SUMS(6),SOUTH(6),GLOBAL(6)
DO 18 J=1,6
WEIGHT=0.0
H=0.0
SUMN(J)=0.0
DO 19 I=1,9
WEIGHT=WEIGHT+(SIN(3.14/2.-H)-SIN((8.+3.14/18.)-H))
SUMN(J)=SUMN(J)+(X(I,J)*(SIN(3.14/2.-H)-SIN((8.+3.14/18.)-H)))
19 H=H+(3.14/18.)
NORTH(J)=SUMN(J)/WEIGHT
WRITE(6,101)NORTH(J)
101 FORMAT(" ",*THE NORTHERN HEMISPHERICAL WEIGHTED AVERAGE FOR
1 THE QUANTITY NOTED ABOVE IS",F10.3)
18 CONTINUE
DO 20 J=1,6
WEIGHT=0.0
H=0.0
SUMS(J)=0.0
DO 21 I=10,18
WEIGHT=WEIGHT+(SIN(3.14/18.+H)-SIN(H))
SUMS(J)=SUMS(J)+(X(I,J)*(SIN(3.14/18.+H)-SIN(H)))
21 H=H+(3.14/18.)
SOUTH(J)=SUMS(J)/WEIGHT
WRITE(6,102)SOUTH(J)
102 FORMAT(" ",*THE SOUTHERN HEMISPHERICAL WEIGHTED AVERAGE FOR
1 THE QUANTITY NOTED ABOVE IS",F10.3)
20 CONTINUE
DO 22 J=1,6
GLOBAL(J)=(SUMN(J)+SUMS(J))/(2.*WEIGHT)
WRITE(6,103)GLOBAL(J)
103 FORMAT(" ",*THE GLOBAL WEIGHTED AVERAGE FOR THE QUANTITY NOTED
1 ABOVE",F10.3)
22 CONTINUE
RETURN
END

```

REFERENCES

- Budyko, M. I., 1970: A Global Climate Model Based on the Energy Balance of the Earth - Atmosphere System. Journal of Applied Meteorology, 8, 310.
- Faegre, A., 1972: An Intransitive Model of the Earth-Atmosphere-Ocean System. Journal of Applied Meteorology, 11, 4-6.
- Lorenz, E. N., 1970: Climate Change as a Mathematical Problem. Journal of Applied Meteorology, 9, No. 3, 325-329.
- Ludwig, J. H., Morgan, G. B., McMullen, T. B., 1970: Eos Trans. American Geophysics Union, 51, 468.
- Ludwig, J. H., McCormick, R. A., 1967: Climate Modification by Atmospheric Aerosols. Science, 156, 1358.
- Mitchell, M. J., 1970: The Problem of Climate Change and its Causes. Man's Impact on Climate. Cambridge, Mass., M.I.T. Press, 133-137.
- Rasool, S. I. and S. H. Schneider, 1971: Atmospheric CO₂ and Aerosols: Effects on Large Increases or the Global Climate. Science, 173, 138-141.
- Schaefer, V. J., 1970: The Measurement of Aerosol Particles on a Global Scale. Man's Impact on Climate. Cambridge, Mass., M.I.T. Press, 364.
- Sellers, W. D., 1973: A New Global Climate Model. Journal of Applied Meteorology, 12, No. 2, 241-254.
- , 1971: Remote Measurement of Pollution NASA sp-285, NASA Langley Research Center, National Aeronautics and Space Administration, Washington, D.C.

ADDITIONAL BIBLIOGRAPHY

- Atwater, M. A., 1970: Planetary Albedo Change due to Aerosols. Science, 1960, (3953), 64-66.
- Byers, H. R., 1959: General Meteorology, N.Y., Toronto, London, McGraw-Hill, 25-44.
- Charlson, R. J., 1969: Climate, the Influence of Aerosols. Journal of Applied Meteorology, 8, 1001-1002.
- Hodge, P. W., 1971: Nature, 229, 549.
- House, F. B. (Project Manager), 1970: The Reduction, Analysis and Interpretation of Radiation Balance Measurements from ESSA Weather Satellites. Final Report, Contract No. E-119-68(IV), GCA Corporation, GCA Technology Division, Bedford, Mass.
- House, F. B., 1965: The Radiation Balance of the Earth from a Satellite. Ph.D. Thesis, Department of Meteorology, University of Wisconsin.
- Junge, C. E., 1970: The Nature and Residence Times of Tropospheric Aerosols. Man's Impact on Climate, Cambridge, Mass., M.I.T. Press, 302-309.
- Landsberg, H. E., 1970: Man-Made Climate Change. Science, 1970, No. 3964, 1265-1274.
- London, J. and Sasamori, T., 1970: Radiative Energy Budget of the Atmosphere. Man's Impact on Climate, Cambridge, Mass., M.I.T. Press, 141-155.
- Mitchell, M. J., 1970: Man's Impact on Climate. Cambridge, Mass., M.I.T. Press, 167-175.
- Mitchell, J. M., 1970: A Preliminary Evaluation of Atmospheric Pollution as a Cause of the Global Temperature Fluctuations of the Past Century. Global Effects of Environmental Pollution.
- Mitchell, J. M., 1971: The Effect of Atmospheric Aerosols on Climate. Journal of Applied Meteorology

- Mitchell, J. M., 1971: The Effect of Atmospheric Particles on Radiation and Temperature. Man's Impact on Climate, Cambridge, Mass., M.I.T. Press, 293-295.
- Raschke, E., and Bandeen, W. R., 1970: The Radiation Balance of the Planet Earth from Radiation Measurements of the Satellite Nimbus II. Journal of Applied Meteorology, 9, 215-238.
- Sellers, W. D., 1969: A Global Climate Model Based on the Energy Balance of the Earth-Atmosphere System. Journal of Applied Meteorology, 8, 392-400.
- Sellers, W. D., 1965: Physical Climatology, Chicago and London, University of Chicago, Press, 65-68.